Natural Environment Research Council

Institute of Geological Sciences

Mineral Reconnaissance Programme Report

A report prepared for the Department of Industry

D. Ostle
Programme Manager
Institute of Geological Sciences
Keyworth,
Nottingham NG12 5GG

No. 45

Mineral investigations near Bodmin, Cornwall

Part 2—New uranium, tin and copper occurrences in the Tremayne area of St Columb Major

INSTITUTE OF GEOLOGICAL SCIENCES

Natural Environment Research Council

Mineral Reconnaissance Programme

Report No. 45

Mineral investigations near Bodmin, Cornwall

Part 2—New uranium, tin and copper occurrences in the Tremayne area of St Columb Major

Geochemistry
B. C. Tandy, MSc

Geology
B. R. Mountford, BSc,

Mineralogy
I. R. Basham, BSc, PhD

Data treatment
R. C. Jones, BSc

Edited by
U. McL. Michie, BSc

London 1981

A report prepared for the Department of Industry

Mineral Reconnaissance Programme Reports

1 The concealed granite roof in south-west Cornwall

2 Geochemical and geophysical investigations around Garras Mine, near Truro, Cornwall

3 Molybdenite mineralisation in Precambrian rocks near Lairg, Scotland

4 Investigation of copper mineralisation at Vidlin, Shetland

5 Preliminary mineral reconnaissance of Central Wales

6 Report on geophysical surveys at Struy, Inverness-shire

7 Investigation of tungsten and other mineralisation associated with the Skiddaw Granite near Carrock Mine, Cumbria

8 Investigation of stratiform sulphide mineralisation in parts of central Perthshire

9 Investigation of disseminated copper mineralisation near Kilmelford, Argyllshire, Scotland

10 Geophysical surveys around Talnotry mine, Kirkcudbrightshire, Scotland

11 A study of the space form of the Cornubian granite batholith and its application to detailed gravity surveys in Cornwall

12 Mineral investigations in the Teign Valley, Devon. Part 1—Barytes

13 Investigation of stratiform sulphide mineralisation at McPhun's Cairn, Argyllshire

14 Mineral investigations at Woodhall and Longlands in north Cumbria

15 Investigation of stratiform sulphide mineralisation at Meall Mor, South Knapdale, Argyll

16 Report on geophysical and geological surveys at Blackmount, Argyllshire

17 Lead, zinc and copper mineralisation in basal Carboniferous rocks at Westwater, south Scotland

18 A mineral reconnaissance survey of the Doon–Glenkens area, south-west Scotland

19 A reconnaissance geochemical drainage survey of the Criffel–Dalbeattie granodiorite complex and its environs

20 Geophysical field techniques for mineral exploration

21 A geochemical drainage survey of the Fleet granitic complex and its environs

22 Geochemical and geophysical investigations north-west of Llanrwst, North Wales

23 Disseminated sulphide mineralisation at Garbh Achadh, Argyllshire, Scotland

24 Geophysical investigations along parts of the Dent and Augill Faults

25 Mineral investigations near Bodmin, Cornwall. Part 1–Airborne and ground geophysical surveys

26 Stratabound barium-zinc mineralisation in Dalradian schist near Aberfeldy, Scotland: Preliminary report

27 Airborne geophysical survey of part of Anglesey, North Wales

28 A mineral reconnaissance survey of the Abington–Biggar–Moffat area, south-central Scotland

29 Mineral exploration in the Harlech Dome, North Wales

30 Porphyry style copper mineralisation at Black Stockarton Moor,south-west Scotland

31 Geophysical investigations in the Closehouse–Lunedale area

32 Investigations at Polyphant, near Launceston, Cornwall

33 Mineral investigations at Carrock Fell, Cumbria. Part 1–Geophysical survey

34 Results of a gravity survey of the south-west margin of Dartmoor, Devon

35 Geophysical investigation of chromite-bearing ultrabasic rocks in the Baltasound–Hagdale area, Unst, Shetland Islands

36 An appraisal of the VLF ground resistivity technique as an aid to mineral exploration

37 Compilation of stratabound mineralisation in the Scottish Caledonides

38 Geophysical evidence for a concealed eastern extension of the Tanygrisiau microgranite and its possible relationship to mineralisation

39 Copper-bearing intrusive rocks at Cairngarroch Bay, south-west Scotland

40 Stratabound barium-zinc mineralisation in Dalradian schist near Aberfeldy, Scotland: Final report

41 Metalliferous mineralisation near Lutton, Ivybridge, Devon

42 Mineral exploration in the area around Culvennan Fell, Kirkcowan, south-western Scotland

43 Disseminated copper-molybdenum mineralisation near Ballachulish, Highland Region

44 Reconnaissance geochemical maps of south Devon and Cornwall

45 Mineral investigatons near Bodmin, Cornwall. Part 2 — New uranium, tin and copper occurrences in the Tremayne area of St Columb Major

The Institute of Geological Sciences was formed by the incorporation of the Geological Survey of Great Britain and the Geological Museum with Overseas Geological Surveys and is a constituent body of the Natural Environment Research Council

Bibliographical reference
Tandy, B. C. and others. 1981. Mineral investigations near Bodmin, Cornwall. Part 2-New uranium, tin and copper occurrences in the Tremayne area of St Columb Major. *Mineral Reconnaissance Programme Rep. Inst. Geol. Sci.*, No. 45

Photocopied in England for the Institute of Geological Sciences by Four Point Printing

CONTENTS

FIGURES

SUMMARY

Investigations of radiometric anomalies 2 km north-east of St Columb Major, Cornwall, indicate that at the main (Tremayne) occurrence a body containing 600 to 1000 tonnes of uranium at a grade of 0.2 % U may exist within 60 m of the surface. A tin stockwork, similar to the nearby Mulberry and Prosper mines, may be indicated, but tin values are erratic.

The surface radiometric anomalies (150 μR/h maximum) lie in close proximity in an area of altered Lower Devonian calc-silicate rocks and slates, and trend north to south. The largest anomaly measures 600 m by 170 m at the outer (15 μR/h) contour. Radiometric reconnaissance and gridding outlined three main groups of surface anomalies greater than 15 μR/h. The individual anomalies are well defined and isolated, and are contained in an area 1.2 km by 0.7 km. They probably represent separate but related mineralised zones located where northerly oriented structures intersect the easterly trending boundary between calc-flintas and slates.

Soil and trench samples have high uranium, tin, copper and zinc contents. Deep trenches showed extensively altered rocks cut by generally sub-vertical northerly trending quartz veins and fractures rich in radioactive iron and manganese oxides. A few flakes of meta-torbernite on joint faces were exposed in one narrow fissure.

Two inclined boreholes were drilled to examine the largest radioactive structure. Core recovery was poor, and technical problems led to both boreholes being stopped before reaching their intended depths. Meta-autunite and meta-torbernite occur at true depths of 34 to 38 m in the first borehole core and 18 to 29 m and 34 to 36 m in the second. Analytical and gamma log data indicate broad zones of moderate grade uranium. A maximum of 0.2 % U over a core length of 3 m is the conservatively assessed value in the second borehole. Copper, zinc, cobalt and tin values are also high, and further drilling is recommended.

INTRODUCTION

A uranium reconnaissance programme in south-west England, undertaken by the Institute of Geological Sciences and sponsored by the United Kingdom Atomic Energy Authority, included a carborne scintillation counter survey of parts of north and mid-Cornwall in April/May 1972 (Tandy, 1974). Anomalies were recorded near Tremayne Farm, National Grid Reference SW 9385 6475, about 3 km north-east of St Columb Major (Figures 1, 2 and 3).

Investigation of the anomalies included radiometric reconnaissance and gridding, shallow auger drilling, soil sampling, sampling of radon in soil air, trenching and deep core drilling at various periods between May 1972 and November 1974. The Department of Industry Mineral Reconnaissance Programme supported the investigations from April 1973 onwards, because of the multi-element association of tin, copper and cobalt with uranium.

GENERAL GEOLOGY

An easterly trending periclinorium, made up of the Dartmouth Beds in the core succeeded by the Meadfoot Beds, both of Lower Devonian age, underlies the St Columb Major area (Ussher, Barrow and MacAlister, 1909). The outcrop of the Dartmouth Beds widens westwards from St Columb to the coast, and the remainder of the area is occupied by the Meadfoot Beds. Both groups consist mainly of slates, for which the local term 'killas' is used.

Dykes, sills and bosses of 'greenstone' (altered dolerites) traverse the area and just pre-date the granite. These units, mostly following the strike of the country rock, have been a controlling factor in localising enrichment of uranium and base metals elsewhere in Cornwall such as at South Terras. The St Austell granite, of Variscan age, exhibits a variety of metasomatic effects. Two small satellite granite intrusions at Castle-an-Dinas and Belowda Beacon lie 4 km east of St Columb (Figure 2). The last major tectonic event occurred during the Alpine orogeny, when south-west England underwent large scale dislocation along north-westerly oriented dextral wrench faults (Dearman, 1963), which may traverse the St Columb area.

The scheme of mineral zonation in Cornwall (Dewey, 1925), suggests that the St Columb area should lie within the lower temperature zones, in which uranium may be emplaced. Metals commonly associated with uranium in low temperature suites in Cornwall, such as cobalt, nickel, bismuth and

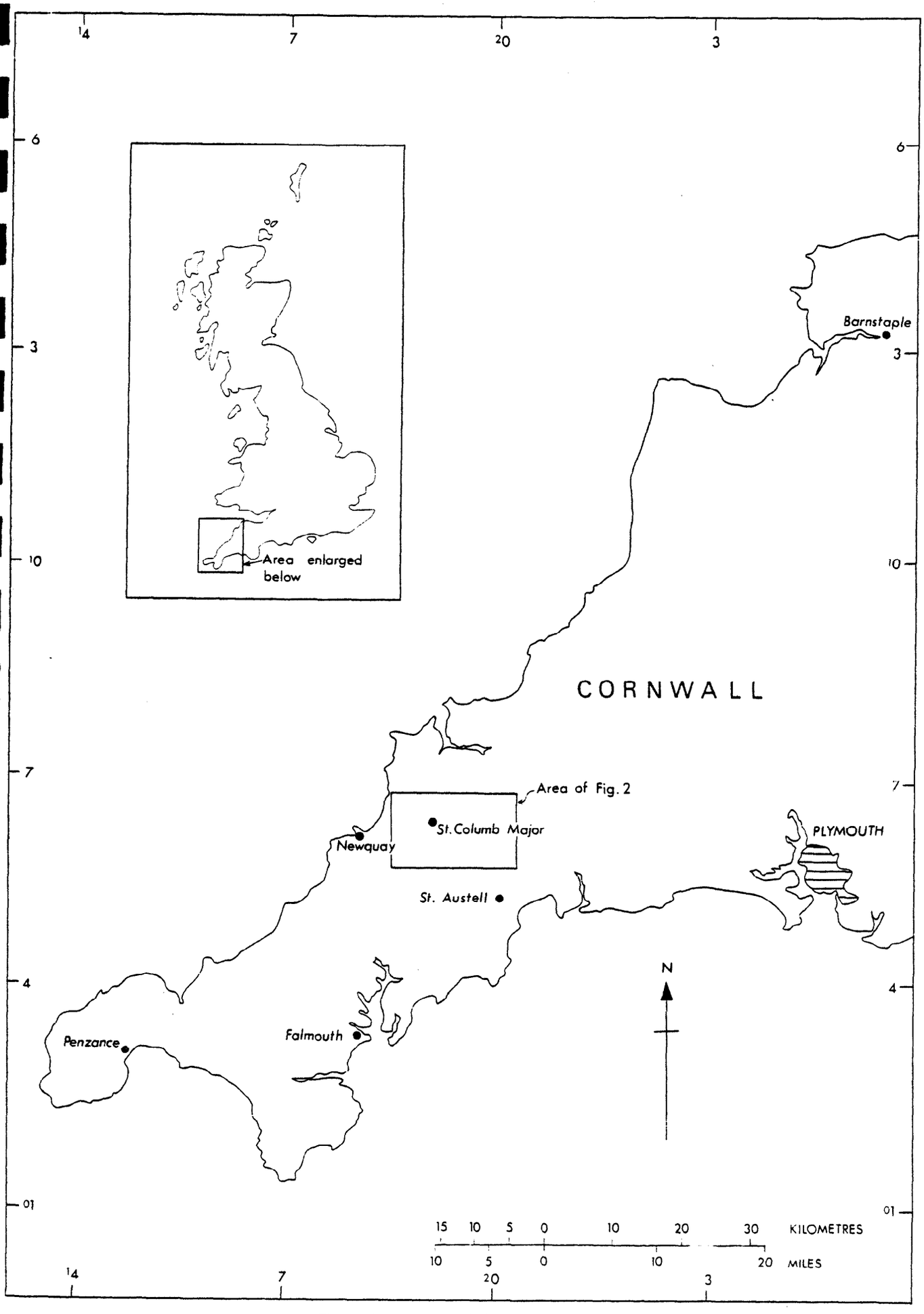

Figure 1. Location of St. Columb Major.

iron, have been mined in the area (Figure 2), along with other metals such as tin, lead, copper, tungsten and manganese (Dines, 1956).

LOCAL GEOLOGY

The area east of St Columb is underlain by interbedded calc-silicate rocks (calc-flintas), grey silty slates and finely argillaceous slates of the Meadfoot Beds (Figure 2). The calc-silicate rocks were originally laid down as siliceous marls mixed with calcareous sands and basic tuffaceous igneous detritus in a marine sedimentary environment, and have since undergone considerable metasomatic alteration. Ubiquitous slaty intercalations undoubtedly represent co-depositional carbonate-poor argillaceous siltstones and mudstones.

Banded green, yellow and white, mainly fine-grained calc-silicate rocks are readily recognisable in hand specimen, and under the microscope they display a wide range of mineral content. Quartz and albitic plagioclase feldspar are common within the more silicic lenses, whilst the more calcic lenses are represented by pale green diopside-hedenbergite with fibrous laths of actinolite-tremolite, anomalously birefringent clinozoisite-epidote and chlorite, weakly birefringent grossularite and interlocking grains of somewhat anomalously birefringent idocrase. Abundant axinite and rare tourmaline indicate the widespread boron metasomatism which these rocks have undergone. Axinite is usually present as an aggregate of interlocking lath-like crystals either as a component of the calcic lenses or as cross-cutting veinlets. Sub-rounded detrital zircon crystals are particularly common in some lenses. Secondary magnetite also occurs as an accessory mineral in most thin sections.

Evidently the considerable recrystallisation displayed in the calc-silicate assemblages is a result of moderate grade thermal metamorphism, accompanied or followed by extensive boron metasomatism. Both phenomena are presumably related genetically to the intrusion of the nearby St Austell granite. The metamorphic grade attained by these calc-silicate rocks is apparently higher than that of the associated grey slates. Thus, the calc-silicate rocks, which form a belt 1.5 km wide stretching 16 km from St Columb Major to Lanhydrock, represent a distinctive unit within the local geology.

Throughout much of the calc-silicate outcrop there is a pronounced steep ($\sim 60°$) northerly dip and E-W strike but at Tremayne the beds exhibit a consistently southerly dip. Microfoliations, kink-banding and crenulation cleavage are evident in thin section, especially within the more argillaceous lenses. Such multiphase deformation is further supported by variations of bedding and cleavage attitude in the drill core, but uncertainties of orientation preclude detailed structural interpretation.

MacAlister (in Ussher and others, 1909, p. 92) suggests that the complex northern outcrop of calc-silicate rocks forms part of the northern limb of the Watergate Bay anticline, whose E-W axis passes through the Belowda Beacon and Castle-an-Dinas granite outcrops. It must be presumed that the metamorphic and metasomatic effects derive from the buried portion of the granite outcropping some 2 km to the south. If it seems unlikely that the marked thermal changes could have been produced at sites so distant from the igneous contact, then it may be necessary to consider transportation of the metamorphic/metasomatic bodies to their present site from a former position closer to the granite. A possible mechanism could be that of a low-angle northerly directed series of slides induced by the lateral shouldering effects of the up-rising pluton – a form of translation invoked by Freshney (1965) to explain metamorphic and structural anomalies at Boscastle.

At Tremayne the outcrop of calc-silicate rocks is marked by a broad E-W ridge which attains a maximum elevation of about 150 m OD. This is crossed by a shallow N-S depression roughly coincident with the radiometric anomaly. The 129 m ?Pliocene marine erosion platform is represented by a small stretch of boggy moorland below and to the north of the site. Over non-mineralised ground the soil is a medium brown, clayey loam with some sand and many angular fragments of banded calc-silicate rock, slate and white quartz. Close to the mineralised zone the soil colour becomes distinctly red and amongst the rock fragments may be found smoky quartz, red and specular hematite and mamillary black manganese oxide. On the ridge crest the combined depth of soil and sub-soil is about 1.0 m and this is underlain by 3 to 4 m of head. The slates and calc-silicate rocks beneath are highly weathered and fractured and commonly exhibit widespread limonitic staining.

SURFACE RADIOMETRIC INVESTIGATIONS

TREMAYNE ANOMALY

Radioactivity was measured at 2 m intervals on approximately east-west grid lines, 10 m apart, over the anomalous areas, using 1413A rate-meters calibrated in μR/hr (100 μR/hr $\approx$ 130 ppm U in equilibrium on a large planar outcrop). The anomalous area, 600 m by 170 m, is crescentic in plan (Figure 4). Background radioactivity was taken as less than 15 μR/hr. The westerly veer of the extremities of the anomaly may be due to: (a) a cut-off on the north-eastern side by north-west trending and bifurcating faults, indicated by some displaced soil radon maxima; (b) the topographic effect, on a westerly dipping structure, of higher ground at the centre and lower ground to the north and south; (c) the structures being arcuate in plan; or (d) the shape reflecting a

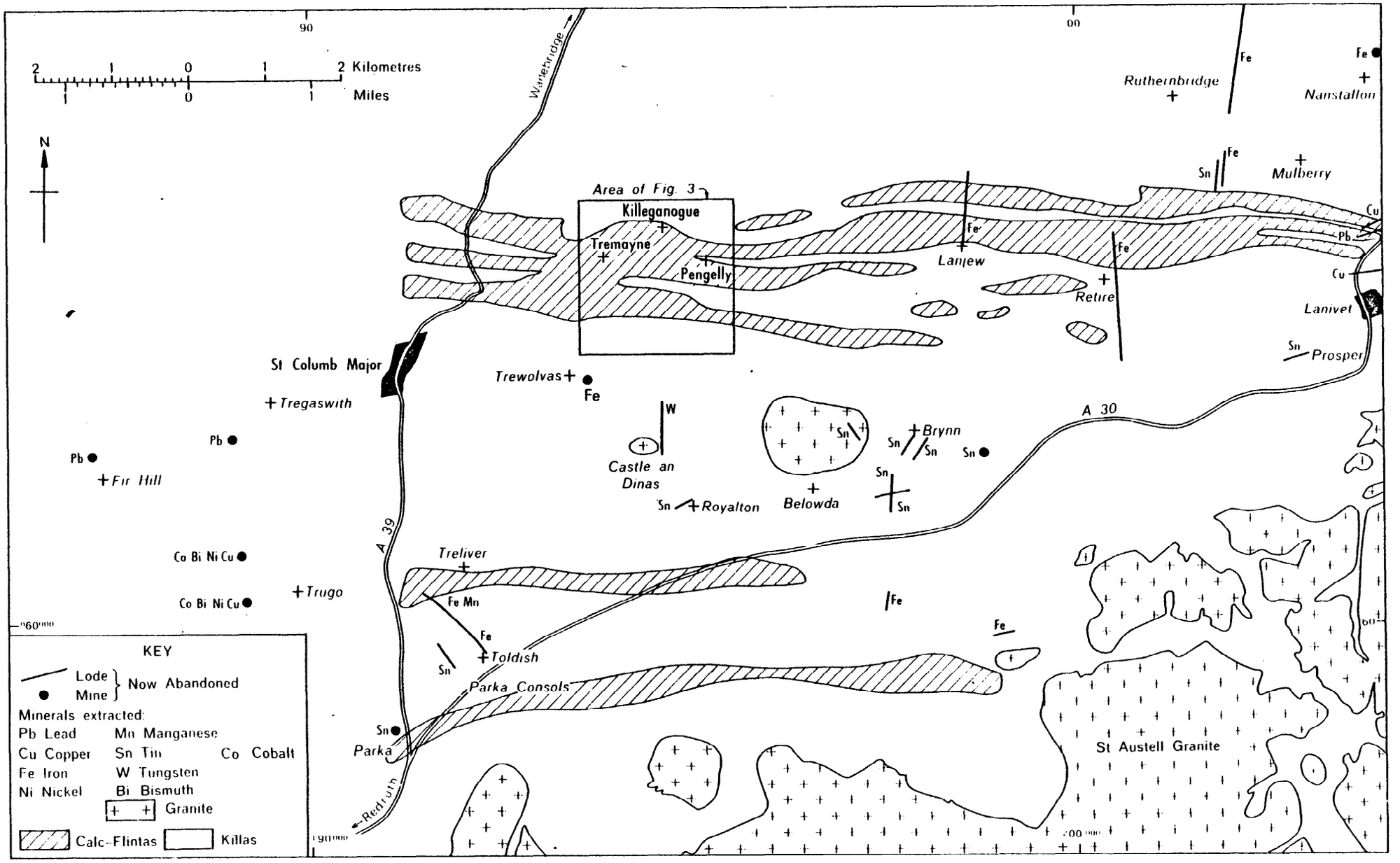

Figure 2. Mineral lodes and former mines in the St. Columb Major area

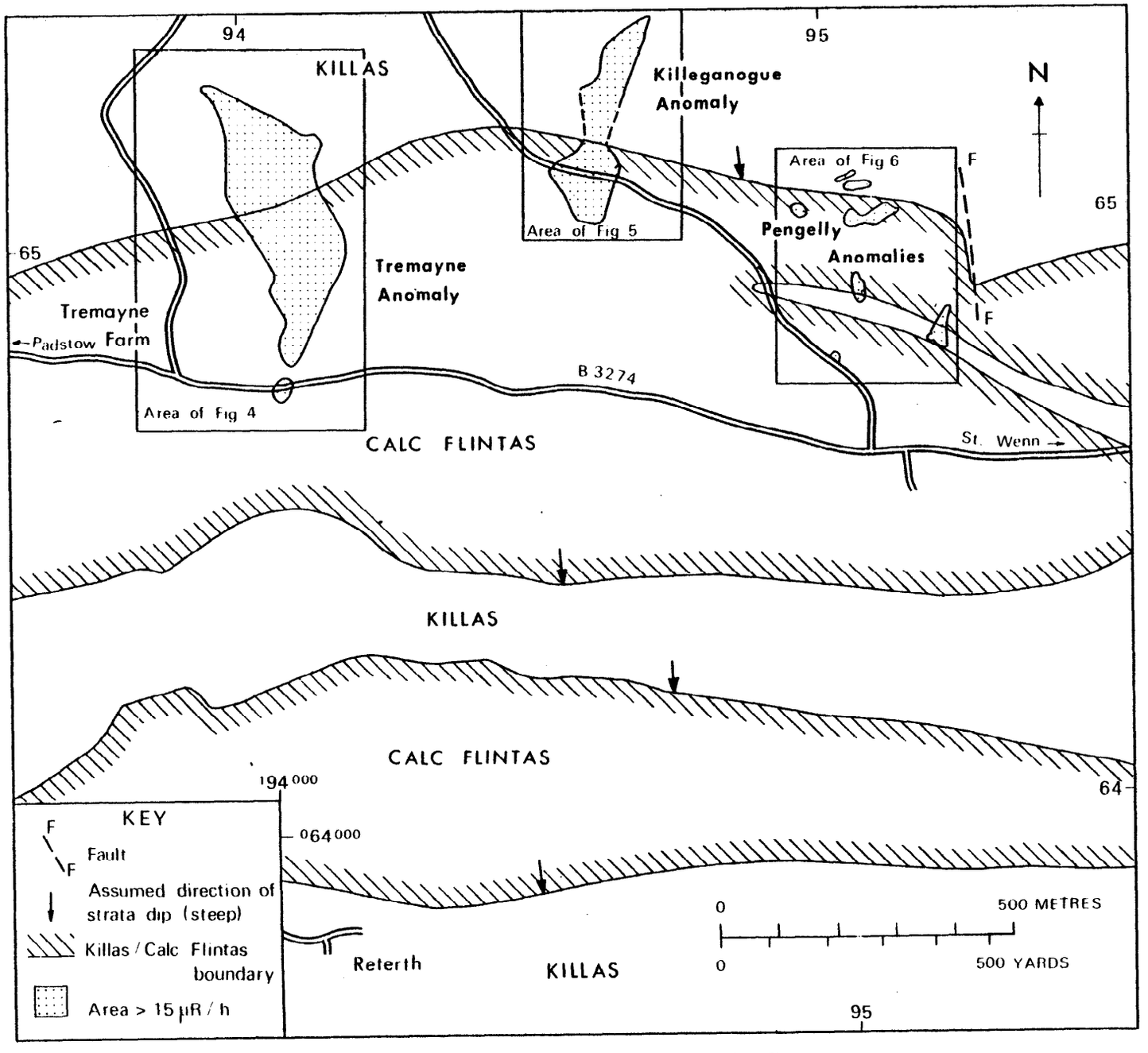

Figure 3. Geology and radiometric anomalies in the Tremayne area

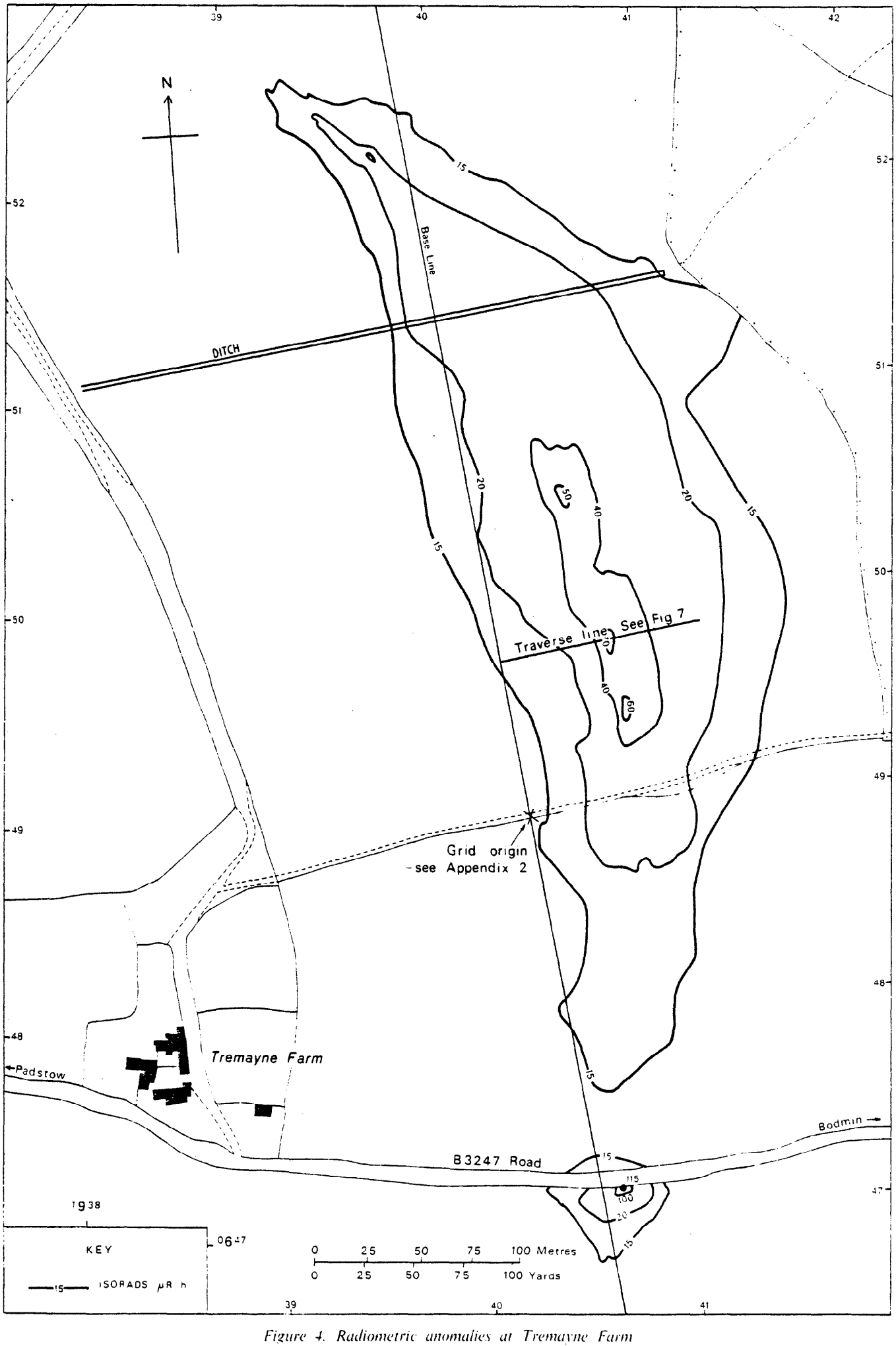

Figure 4. Radiometric anomalies at Tremayne Farm

relationship between mineralisation and folding in the underlying strata.

The symmetry of the isorads indicates a steeply dipping structure. The closure of the isorads at the northern end may be due partly to the burying of the radioactive structure beneath an increasing cover of superficial material (valley gravels).

At the southern end, low surface radioactivity of < 15 μR/h and absence of anomalous radon in soil air isolate the small roadside anomaly from the main anomaly, and may reflect the presence of a band in the underlying strata inhospitable to mineralisation. Mechanical auger drill tailings from this zone were of relatively unaltered regolith, compared with ferruginous and hydrothermally altered clay products from within the radiometric anomalies. To the south of the roadside anomaly, however, soil radon sampling indicates that the radioactive structure continues beneath superficial cover, although with a south-westerly trend.

A slight asymmetry in the central and most radioactive part of the structure, where the isorads on the eastern side of the surface anomaly are more widely spaced, implies that the structure may dip slightly to the east. This is reflected in a profile of a surface gamma and radon in soil air traverse (Figure 7). The radon maximum is offset 35 m east of the surface gamma maximum and coincides with the junction of impermeable hydrothermally altered clays to the east overlying sands a little to the west. Thus radon may be migrating upwards from the radioactive structure through the sands to the lower boundary of the clays. A similar but more subdued feature occurs just ten metres west where another radon peak corresponds with a junction with clays.

KILLEGANOGUE ANOMALY

This anomaly (Figure 5), 370 m by 120 m maximum, > 15 μR/h, has three small isolated maxima within the anomalous area: 45 μR/h in the north; 150 μR/h at 80 m further south; and 75 μR/h at the widest part.

The anomaly widens on the higher ground, south of the break of slope at the mapped calc-flintas/slate boundary (Figure 3). The structure is oriented roughly north-north-east, but, as at Tremayne, some of the isorads have a crescentic form, although with a trend to the east (Figure 5).

Soil radon sampling indicates that the radioactive structure continues for at least 250 m further north, buried beneath valley gravel. The structure is, however, abruptly truncated to the south of the surface anomaly.

PENGELLY ANOMALIES

Seven small isolated anomalies lie to the north and west of Pengelly Farm (Figure 6). Radiometric gridding only was carried out at these sites.

Significantly, most of the anomalies are in zones mapped as calc-flintas/slate boundaries, along breaks of slope (Figure 3). This coincidence indicates possible lithological control of mineralisation. Spreading of uraniferous material along the easterly trending boundary would account for the elongation of the northern group of anomalies. The southern anomalies are of the more common northerly trend (Figure 6).

The anomalies are of relatively low amplitude, reaching a maximum of 60 μR/h. The maxima occupy a few square metres.

SOIL SAMPLING

Samples were taken: (i) by mechanical auger from depths of 1 to 3 m in deeply weathered zones, which accord roughly with the radioactive areas; (ii) by hand auger from depths up to 60 cm in less weathered intervening zones; (iii) from a 1 m deep trench along the south side of the B3274 road, excavated by the North and Mid Cornwall Water Board for pipe laying; and (iv) from a recently excavated 2 m deep drainage ditch north of Tremayne Farm. Samples were taken at intervals of up to 30 m along lines which made approximate 90 m intersections with, and were perpendicular to, the radiometric grid base line. The samples are broadly comparable and are treated as one group of similar samples. The soil samples were analysed for U, Cu, Pb, Zn, B, Sn, Mn, Fe, Co, Ni, Mo, Ba, V, Cr, Y and Nb (Appendix II).

Uranium content, 277 ppm maximum, in samples corresponds closely to the pattern of surface radioactivity (Figures 8 and 9).

Copper values, up to 990 ppm, are generally highest in the most radioactive zones, especially at the Tremayne anomaly (Figure 8). High values are also associated with a lead and zinc anomaly near the Killeganogue structure (Figure 9).

Highest tin values, 560 ppm maximum, are confined mainly to the Tremayne structure (Figure 8), although they vary greatly. This variability may be due to the lack of mobility of tin from localised sources such as quartz veins, or the patchy concentration of tin as a result of the metasomatic alteration of the calc-flintas. These factors may account for the occurrence of this hypothermal element in an otherwise mesothermal zone. Anomalous values also occur to the south of the Killeganogue structure (Figure 9) at a copper and lead anomaly but tin within the radiometric anomaly is low.

Zinc contents are fairly uniform over extensive areas, possibly because of the high geochemical mobility of zinc in this environment. The maximum is 400 ppm.

Lead values are generally low. The few anomalies, up to 240 ppm, are isolated and show little pattern, although a cluster, accompanied by enhancements of other metals, occurs near the Killeganogue radiometric anomaly (Figure 9).

Figure 5. Killeganogue radiometric anomaly

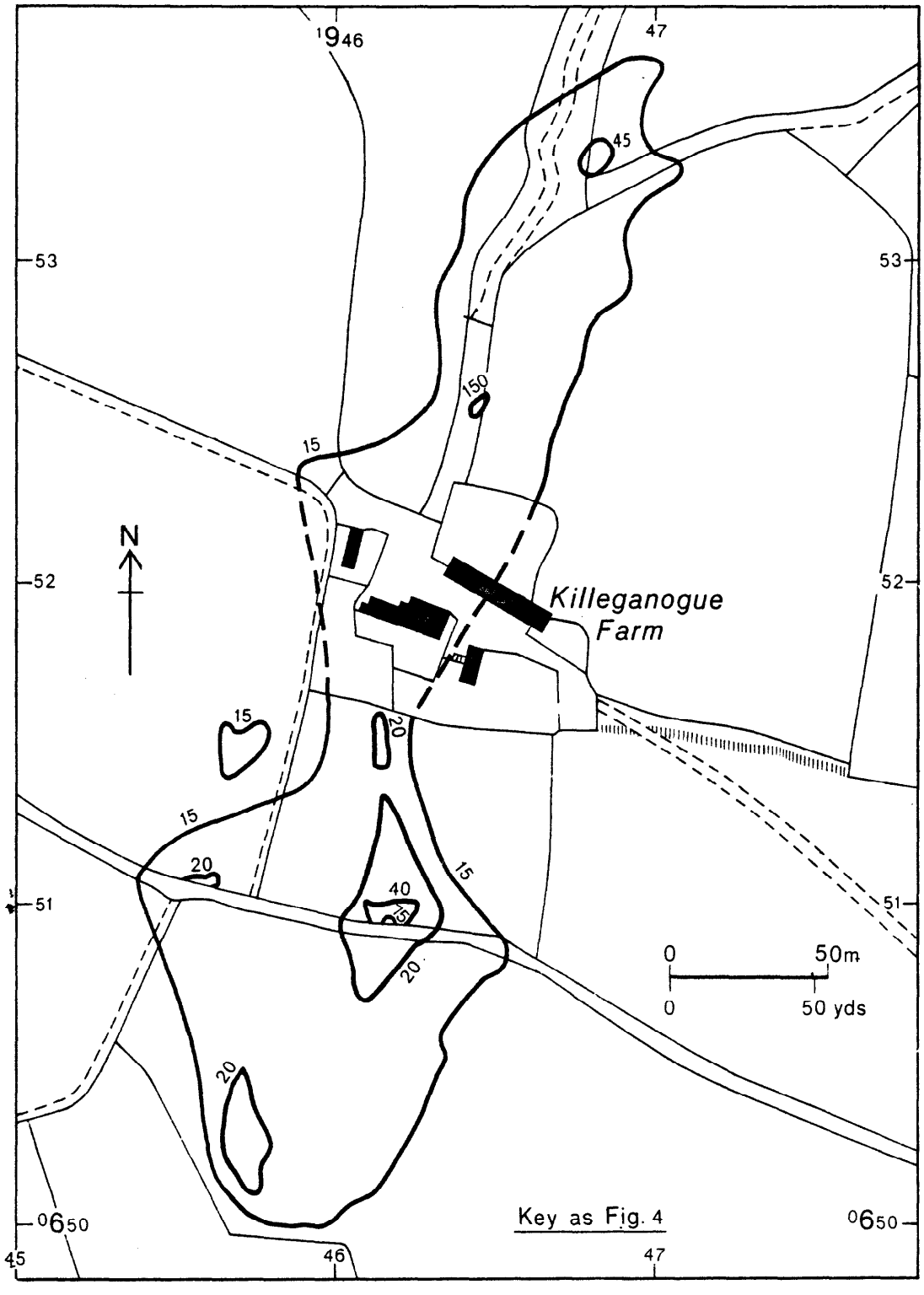

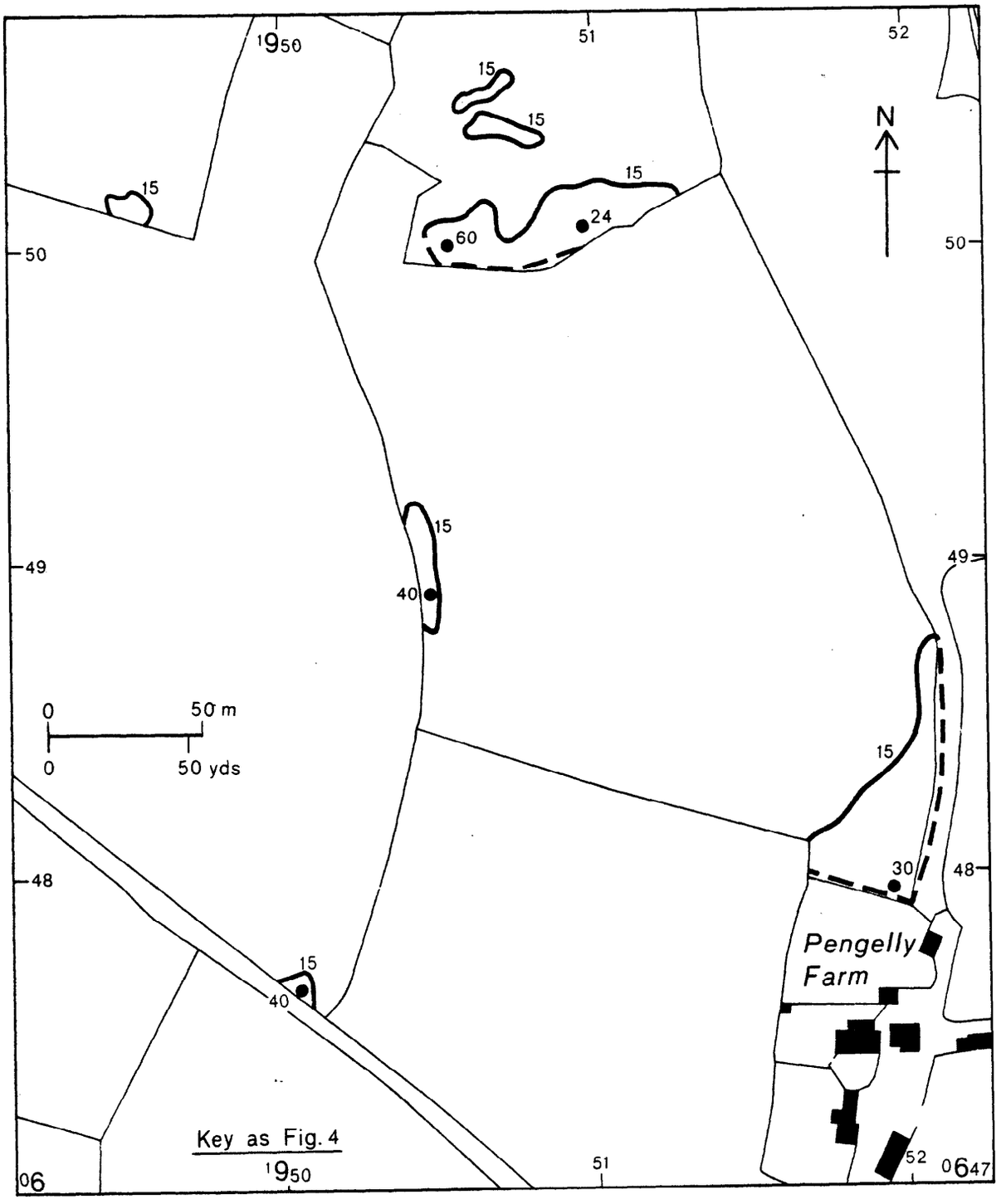

Figure 6. Pengelly radiometric anomalies

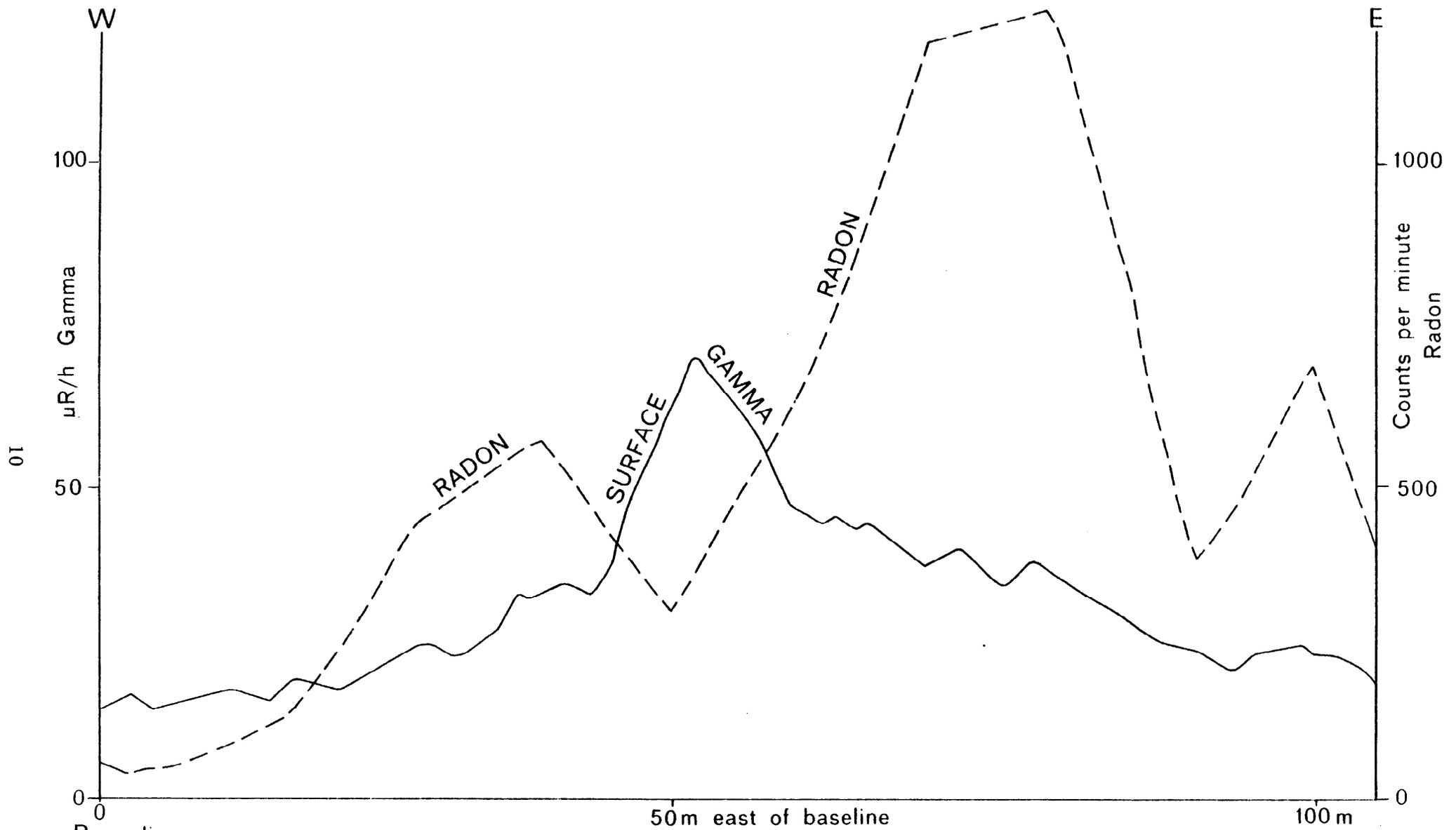

Figure 7. Gamma, and soil radon values across the centre of the Tremayne radiometric anomaly (See Fig. 4)

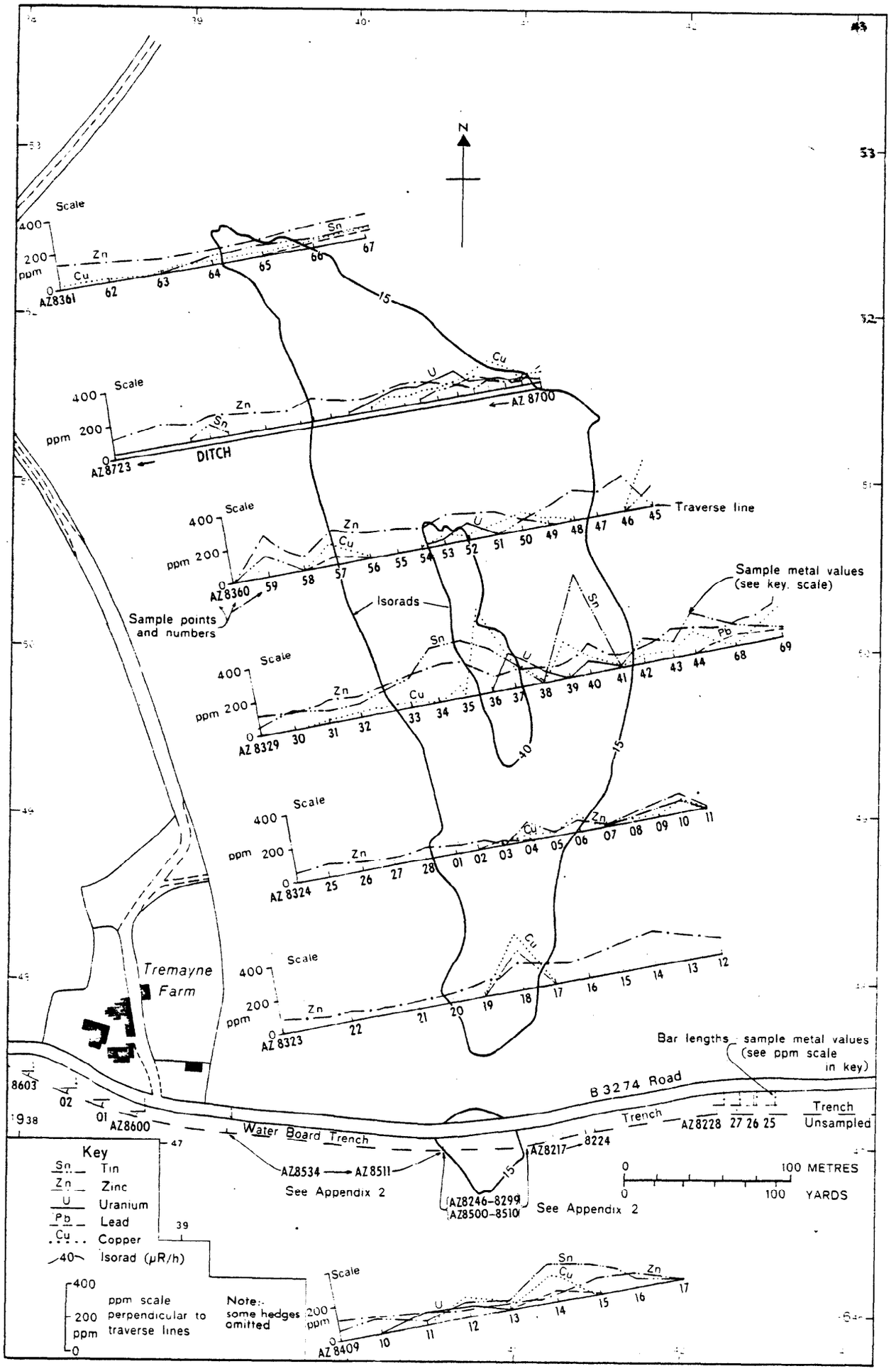

Figure 8. Soil traverses at Tremayne Farm

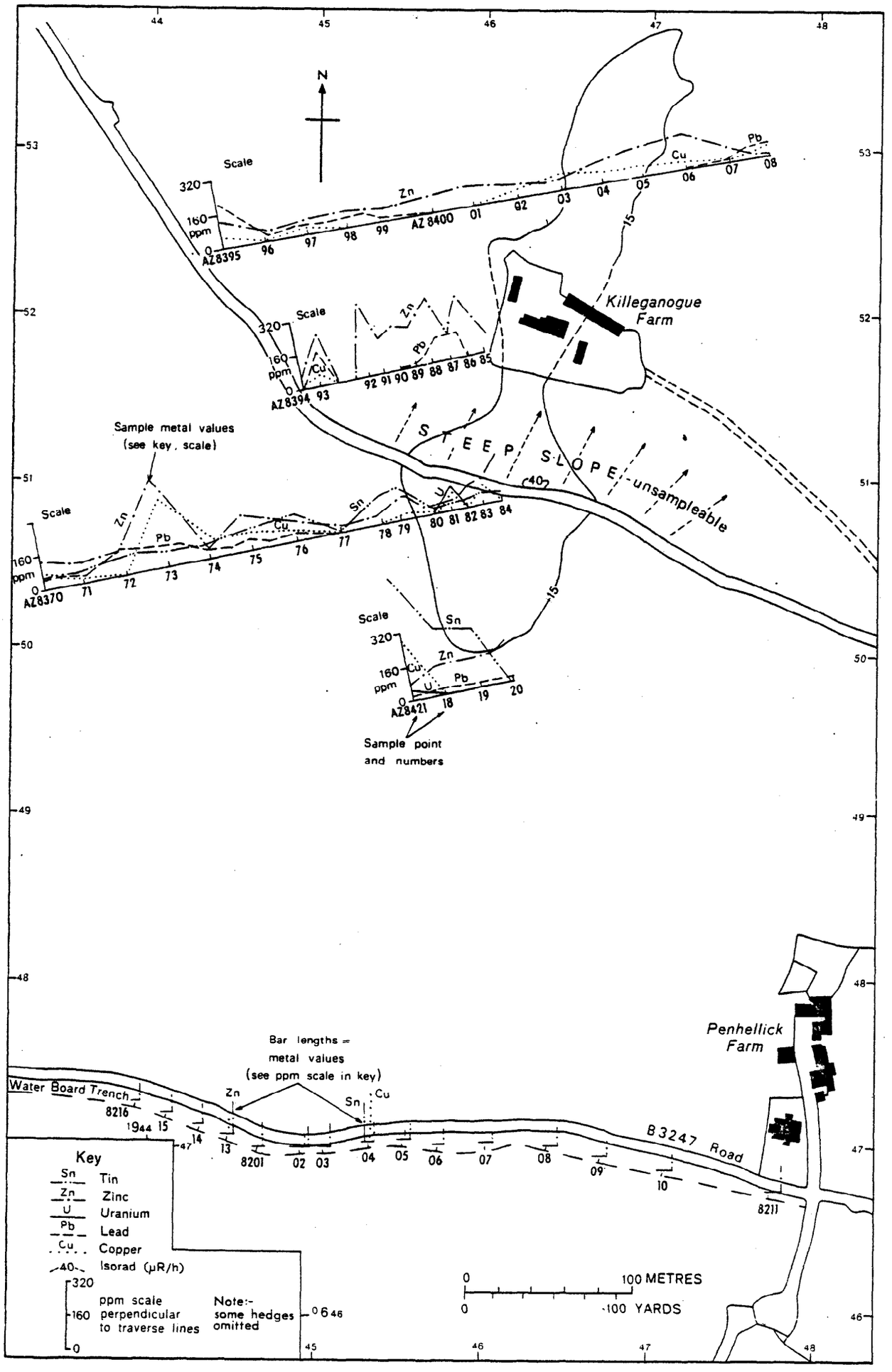

Figure 9. Soil traverses at Killeganogue

TRENCHING

Trenches to a depth of about 4 m were excavated by mechanical digger at the sites of the highest-amplitude soil anomalies. Some of these trenches were extended, and extra trenches were excavated to recross the strike of certain structures (Figures 10 and 11). Samples of weathered rock were collected from the trenches and analysed for the same elements as the soil samples. The analytical results are summarised in Appendix II.

Trenches on the Tremayne structure showed calc-flintas and slate weathered to greenish and yellowish clays with, in places, relict bedding and cleavage. The westernmost 45 m of trench 3 (Figures 12 and 13), corresponding to the highest radioactivity and largest variety of alteration features, was examined and sampled intensively. Other trenches were examined and sampled in less detail (Figure 14).

Two main sets of mineralised fracturing were exposed (Figures 10 and 11). One set has a north-easterly trend, ranges in dip from sub-vertical to 45° to the south-east, and consists mostly of manganese oxide and hematite-stained shatter zones and rarely of quartz veins. The more prevalent set trends northwards, is sub-vertical, and consists mainly of thicker quartz veins and extensive radioactive zones rich in iron and manganese oxides.

Uranium content in the weathered rock samples corresponds to zones of radioactivity. It correlates closely with copper, in zones where quartz veining or iron/manganese oxide-stained and altered calc-flintas predominate. Values reach a maximum of 408 ppm U in a narrow shatter zone containing traces of uranium secondary minerals, in trench A (Figure 14).

High copper contents of 90 to 370 ppm occur in the westernmost 7 m of trench 3 (Figure 12) at a large quartz vein and zone of high radioactivity, and at other points in the trenches generally corresponding to high uranium values. The maximum value, 580 ppm Cu, is in a quartz vein sample from trench A (Figure 14).

Tin contents are at their highest in samples of green clays derived from altered calc-flintas (Figures 13 and 14). A broad zone containing 150 to 943 ppm Sn (maximum) occurs in the eastward extension of trench 3 into trenches 4 and 5, between 35 and 85 m east. Values in other trenches are generally low.

The largest zinc values, 280 to 640 ppm, are in a 5 m zone of limonitic and green altered calc-flintas and clays lying between a manganese/iron oxide-stained structure and a quartz/iron/manganese oxide vein in trench 3 (Figure 13). Other high contents of 100 to 150 ppm Zn occur at isolated points in this trench and in trench A (Figure 14).

Lead tenor is generally low except for a value of 50 ppm in a quartz vein in trench A (Figure 14). Slight enhancement to 20 to 30 ppm Pb are associated with the zinc anomalies in trench 3 (Figure 13).

Mineralogical examination of quartz vein samples shows two colour varieties of quartz. One is clear, and the other is stained grey to red by iron possibly derived from ore minerals with which the quartz is interbanded. Ore minerals, amounting to less than 0.5% of each sample, consist of interstitial hematite, goethite and limonitic material.

Ferruginous vein samples consist almost entirely of the ore minerals mentioned above. Semi-quantitative X-ray fluorescence analysis indicates contents of up to 900 ppm U, 200 ppm Cu, and traces of zinc, arsenic, antimony, strontium, zirconium and yttrium. Autoradiographs exhibit highly-disseminated uranium which is usually adsorbed on grains of iron minerals.

The secondary uranium mineral meta-torbernite (hydrated copper—uranium phosphate) coats the joint faces of a narrow vertical fissure in shattered ferruginous calc-flintas in trench A (Figure 14). Occurrences of this mineral would account for some of the other uranium and copper anomalies.

The main, northerly trending, vein assemblage represents hydrothermal mineralisation chiefly involving the deposition of iron and, by adsorption, uranium. Hematite is a primary ore phase. Adsorption would also account for the other elements detected in trace amounts.

At best, the high tin contents in samples from trenches 3, 4, 5 (Figures 13 and 14) may indicate an orebody similar to some known tin stockworks, such as Mulberry, which occur nearby in similar geological settings. High values are not found in other trenches in the Tremayne area, and this, coupled with the easterly strike and sub-vertical dip of the beds, indicates a possible lithological control for the concentration of tin. Tin may be contained within grossular garnet as reported from Red-a-ven Mine, near Okehampton (El Sharkawi and Dearman, 1966).

Other trenches were generally used to examine the geological setting of the radiometric anomalies, and structural information recorded is shown on Figures 10 and 11. Samples were not collected systematically, and analytical results for the weathered samples collected accord with those already discussed.

DRILLING

Based on the near-surface investigations at Tremayne Farm, two rotary water-flush wire-line cored boreholes were drilled (Figure 15) in October and November 1974. Stratum-controlled tin mineralisation was expected in the northerly oriented borehole 1; and uranium, copper and tin, in a northerly trending structure, was anticipated in the westerly oriented borehole 2. Target depths of 100 m were planned for each. Borehole logs

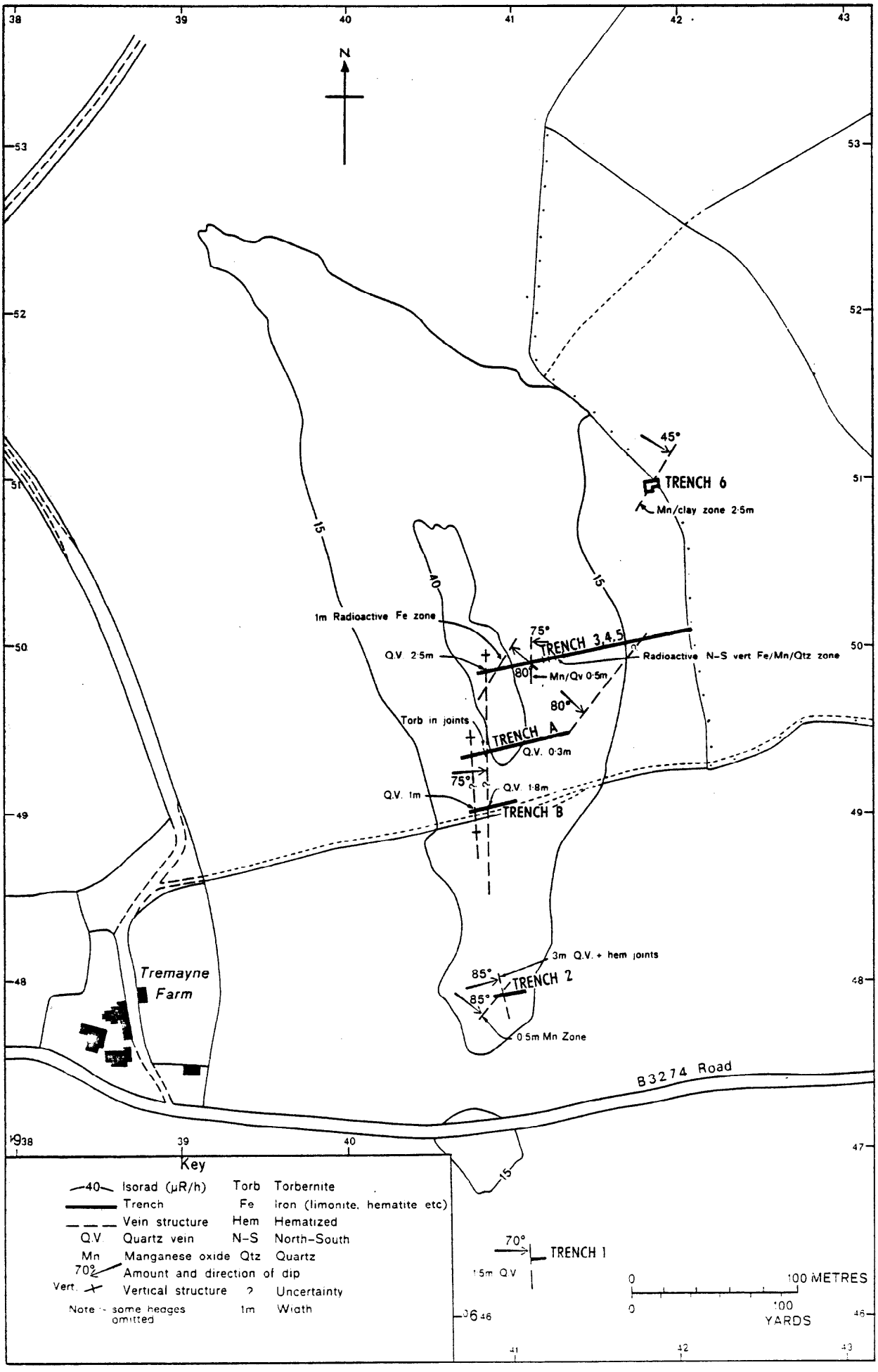

Figure 10. Trenches and structures at Tremayne Farm

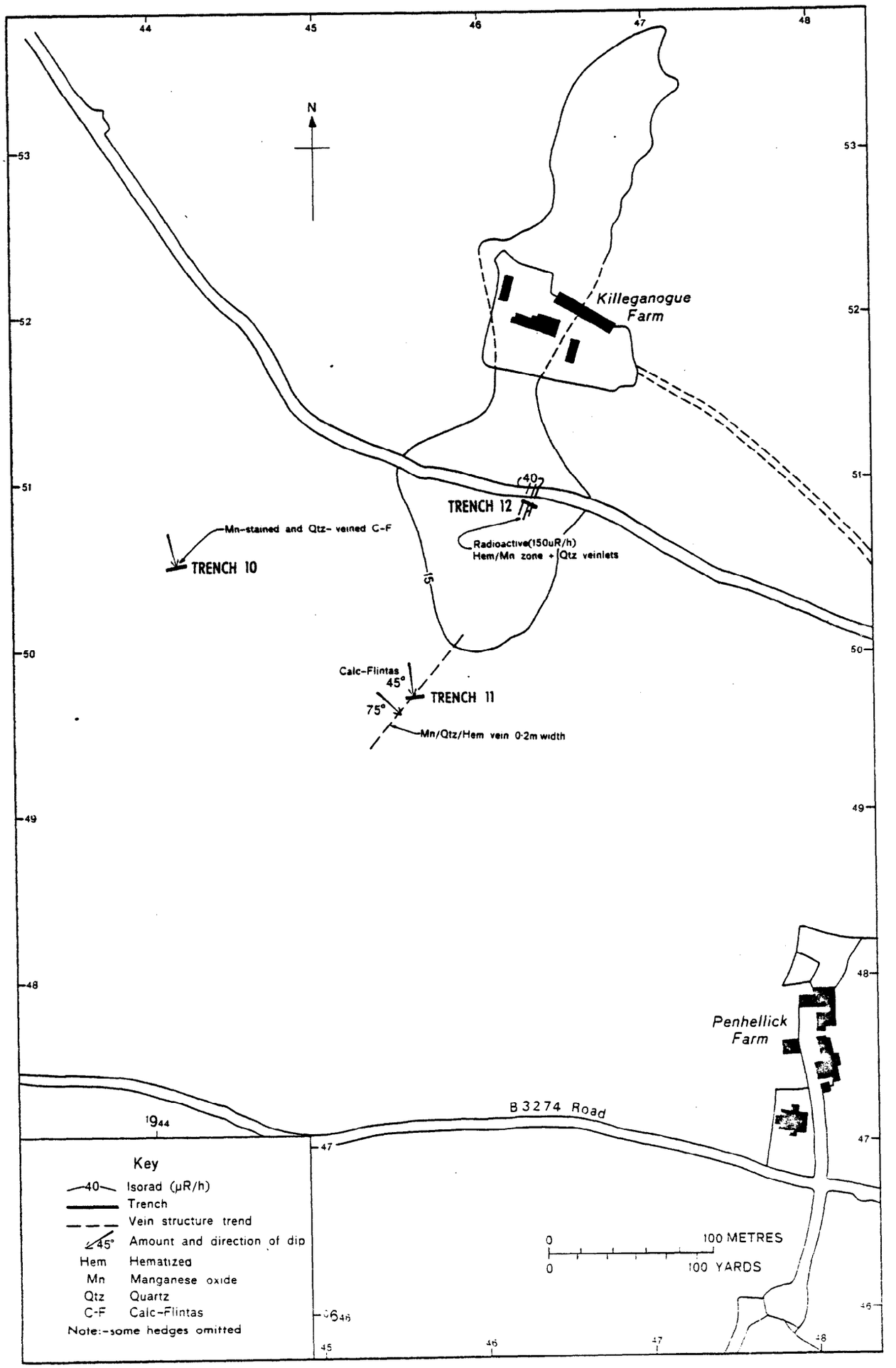

Figure 11. Trenches and structures at Killeganogue

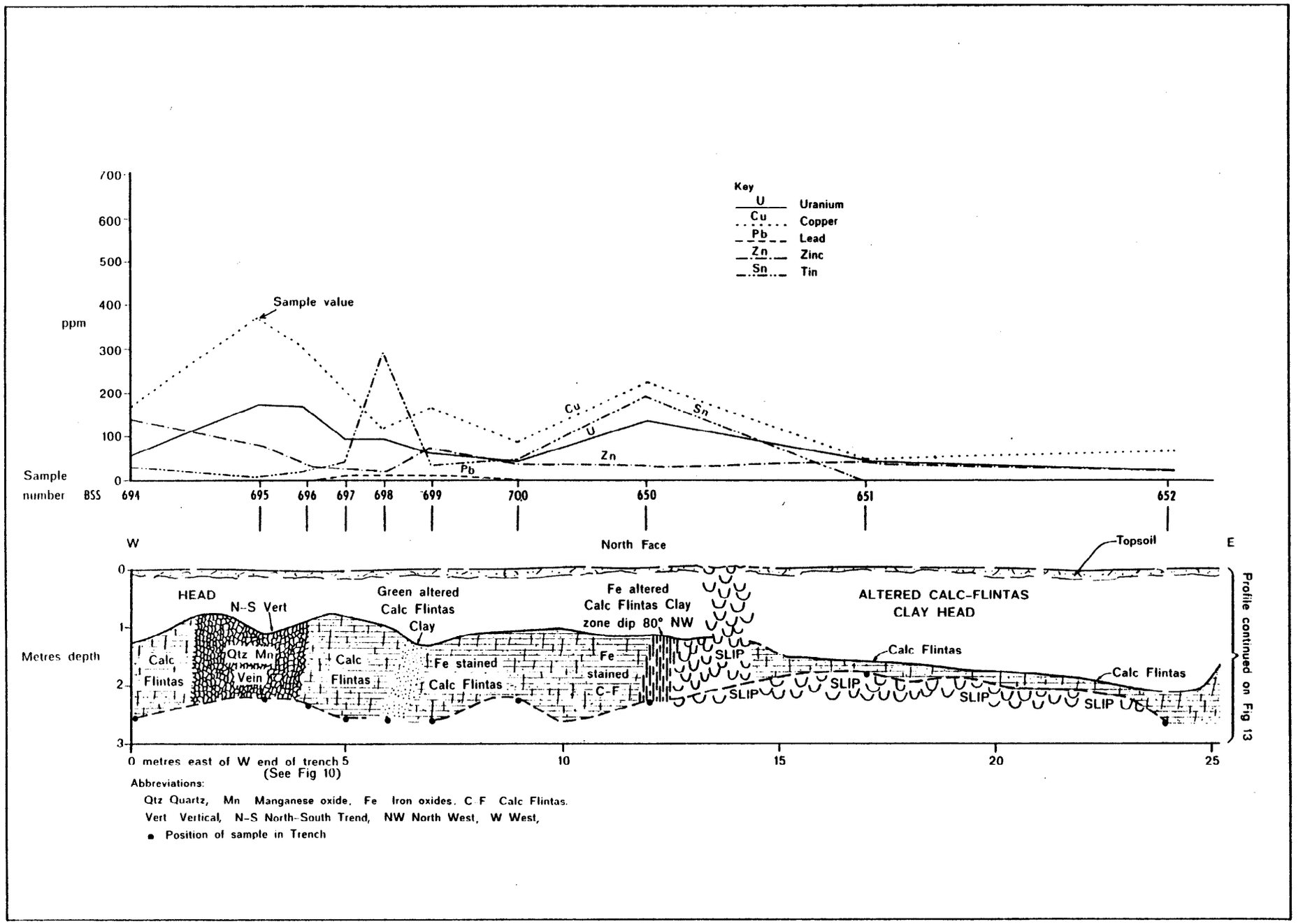

Figure 12. Detailed profile of western end of trench 3, 4, 5

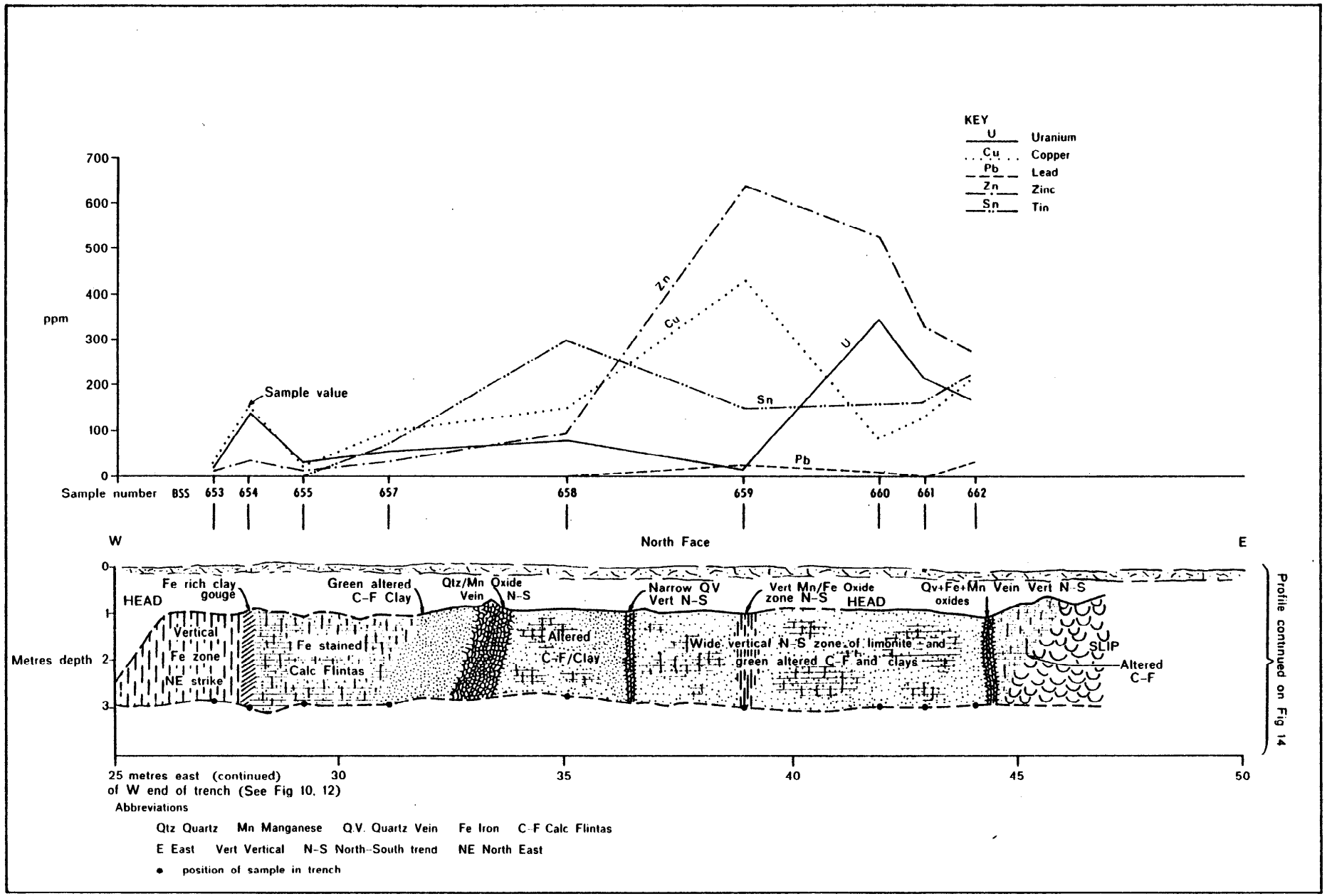

Figure 13. Detailed profile of continuation of trench 3, 4, 5

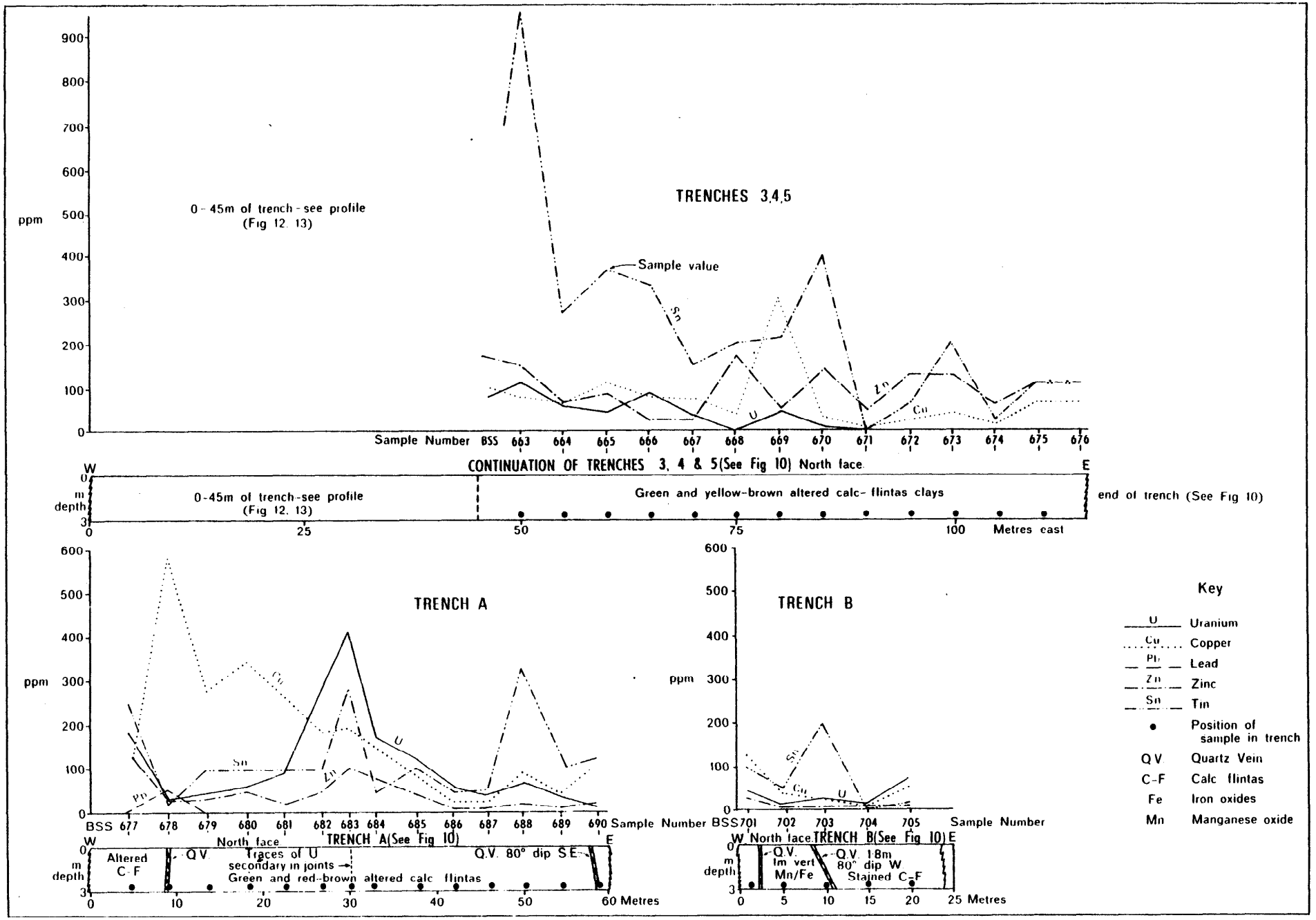

Figure 14. Less detailed profiles of eastern end of trench 3, 4, 5, trench A and trench B.

are given in Appendix I. Figures quoted in the text refer to inclined lengths/depths unless otherwise stated. True depths may be assessed by reference to Figures 16, 17, 18, 19 and Appendix I.

Borehole 1 was aligned azimuth due north, declined at 47°. Within the first day, 29.9 m length was drilled (Figure 16), but with little recovery owing to the decomposition of the rock. The borehole was cased to its intersection with a quartz vein at 28.9 m.

Progress diminished for the remainder of the drilling as fractured quartz vein and decomposed rock below 37.6 m led to excessive wear on bits, loss of water pressure, hole collapse and subsequent loss of cement. Wire-line was used to drill beyond 39.3 m, but serious collapsing in the borehole resulted in curtailment of drilling at a depth of 53.7 m.

Borehole 2 was originally to be located at the site of the first borehole but declined at 45°, azimuth west. In the light of the difficulties encountered in borehole 1, the site for the second was moved 27 m farther west, nearer to the structures to be intersected, so that the declination could be steepened to 60° hopefully to overcome the problems of low angle drilling. The borehole was oriented on an azimuth of 265°. Progress was again initially rapid, and the borehole was cased down to 42.7 m through intensely weathered calc-flintas (Figure 17). Despite the best efforts of the drillers, however, problems similar to those found in the first borehole were encountered and the hole was finally abandoned at 50.5 m.

RADIOMETRIC LOGS

Both boreholes were radiometrically logged (Figures 16 and 17), although borehole 1 could be logged only down to 49 m as drill rods had been temporarily left in to prevent hole collapse. A scintillation probe and then a Geiger-Muller (G-M) probe, connected through a 1368A ratemeter to a 1417A chart recorder, were used to provide the logs.

Borehole 1 logs (Figure 16) reveal several zones of high radioactivity, some where core recovery was poor or non-existent (Appendix I). From the base of the quartz vein at 37.5 m depth to the bottom of the logged portion of the hole at 49 m, the radiation level increases markedly. The gamma level is off the highest scale of the ratemeter/recorder plus scintillation probe from 38.1 to 39.6 m, and 43.6 to 49 m. The G-M probe log shows maxima of 0.04 mR/h at 38.7 m, 0.85 mR/h at 47.3 m, and exceeds 0.4 mR/h down to 49 m.

Borehole 2 logs show a generally higher level of radioactivity (Figure 17), as the radioactive structure was penetrated. The scintillation probe log is off-scale from 9.8 to 11.6 m depth, 16.8 to 38.1 m, and at 47.3 m. The G-M probe log shows maxima reaching 0.3 mR/h from 20.7 to 23.8 m, and 0.95 mR/h from 38.1 to 40.2 m.

The locations of the highest radiometric log values correspond to zones of secondary uranium minerals, comprising meta-autunite with subordinate torbernite in the core fragments which have hematitisation or manganese oxide staining.

ANALYTICAL RESULTS AND ASSESSMENTS

The G-M log values had previously been calibrated at the Grand Junction (USGS) facility, giving 0.4 mR/hr ≈ 0.1% U. Local corrections have to be applied for disequilibrium, hole diameter and thickness of casing. Uranium analyses and equilibrium measurements on recovered core were used to calibrate the gamma logs and to derive assessments of the uranium grade where no cores were retained. As core recovery was poor, however, the analysed samples are not necessarily representative of material intersected by the drill. Core lengths are generally incomplete and fragmented (Appendix I). The grades derived from the logs should therefore be used only as approximate values.

A total of 76 samples were taken from the cores and analysed for the same elements as the soils (Appendix II). Samples represent at least each rock type or a total length recovered on withdrawal of the core barrel. Friable core was channel-sampled, and fragments were selected to represent the lengths of core in which they occur. Where recovery was more complete, representative samples were taken at more precise points in the core, but again some uncertainty exists about exact positions because of core loss. Sample positions are generalised in the text and illustrations and are shown as occurring around a median point in any particular recovered length in the core box.

Sampling was more concentrated in lengths of mineralised core (Figures 16, 17, 18 and 19), so little weight would be attached to average analytical values (e.g. those given in Table 6), with the exception of those for restricted lengths of core, indicated below, where arithmetic means are quoted. Analytical logs of the boreholes are shown in Figures 21 and 22.

Borehole 1

Highest uranium values are clustered towards the base of the borehole, between 48.8 and 54 m depth, where abundant uranium secondary minerals and high radioactivity occur (Figure 16). The mean value in 11 samples is 470 ppm U over a length of 4 m. The highest value is 1232 ppm U.

There is a wide variation of eqilibrium values in the few samples measured. Taking, however, overall equilibrium factors between 1.0 and 2.0 for e U_3O_8 $(\beta + \gamma)$/e U_3O_8 (γ) in samples from 37 to 44.5 m depth (Figure 16), where log values average 0.03 mR/h, mean grade lies between 50 and 200 ppm uranium over a length of 5 m. Between 44.5 and 49 m, using an equilibrium value

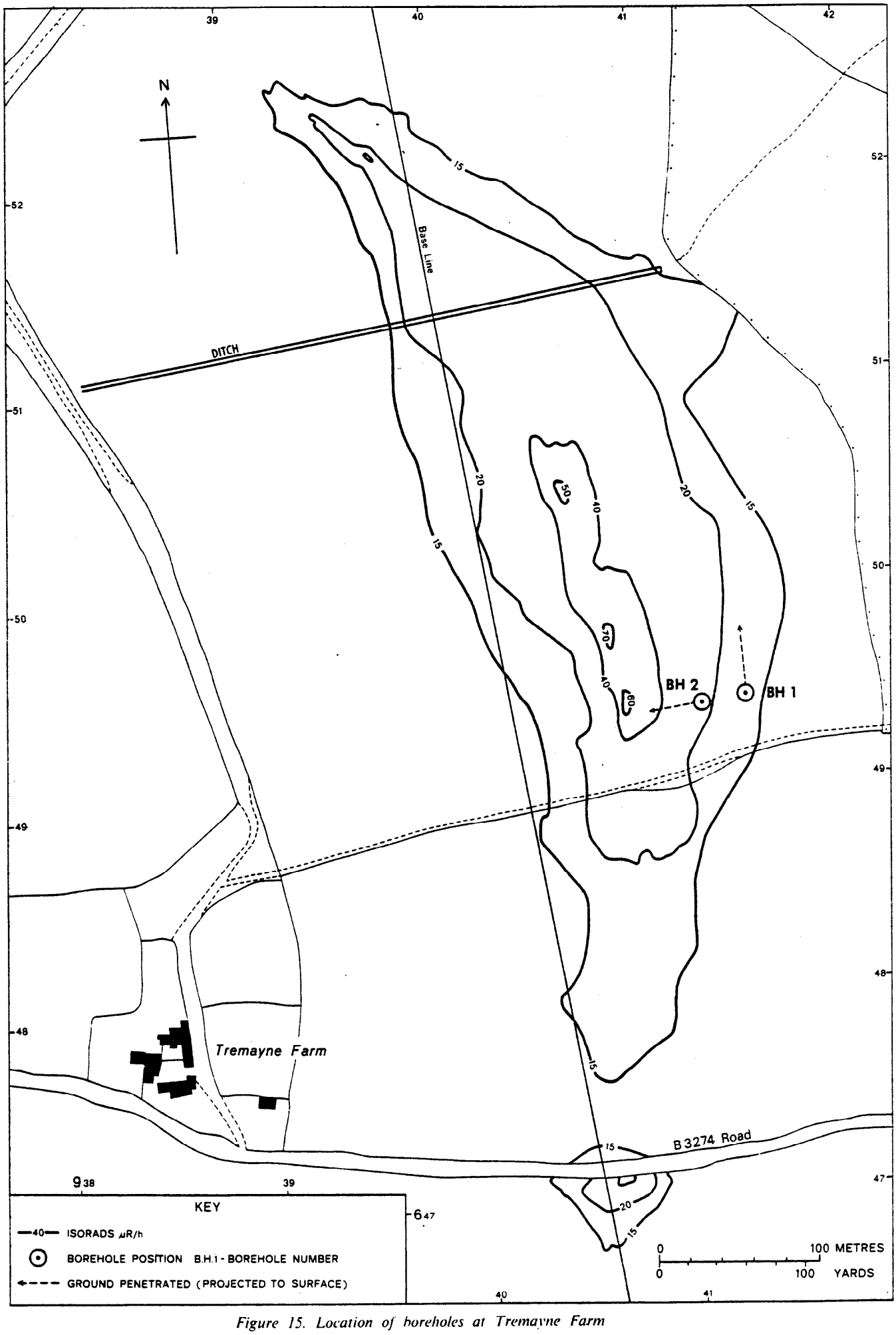

Figure 15. Location of boreholes at Tremayne Farm

of 1.03 and a uranium analysis of 468 ppm in one isolated sample (BSR 1038), in which zone the mean log value is 0.4 mR/h, mean grade is probably about 700 ppm U over a length of 3 m. Maximum grade may be about 1400 ppm U at 47 m, at the gamma peak.

No gamma readings were obtained from the next (and lowest) 5 m of the hole. Analytical values of samples from the core recovered below 49 m, however, correspond closely to the assessed values from the adjacent length. Thus the mean uranium grade probably lies between 500 and 700 ppm over a total length of 7 m at the bottom of the borehole.

These grades are regarded as encouraging, when it is considered that this borehole was drilled northward parallel to and 60 m east of the axis of the surface radiometric anomaly. They could represent the outer margins of a uranium orebody.

Of the other metals (Figure 18), the highest copper tenors occur largely in a thick hematitised quartz vein, in which the mean level is 520 ppm Cu from seven samples over a length of 5 m. This quartz vein, intersected at an acute angle, probably represents a continuation of the quartz vein in trench A (Figures 10 and 14), where it has a width of 0.3 m.

Tin contents are variable. The maximum, 1203 ppm Sn, occurs in clay derived from calc-flintas, at 11.3 m depth. Otherwise, values do not exceed 325 ppm Sn down to a depth of 39 m, at which point a sample from the margin of a quartz vein contains 680 ppm Sn. At 39.3 m depth, 680 ppm Sn was recorded in calc-flintas. Values decrease to below 300 ppm Sn towards the bottom of the borehole, and the overall average grade in the core is only 230 ppm Sn.

Zinc (280 ppm maximum) and lead (80 ppm maximum) show low and irregular values. A mean of 227 ppm Co occurs in four samples from the zone between 49 and 51 m, associated with moderate enhancements of uranium. The highest value is 521 ppm Co.

Borehole 2

High mean values of uranium occur in a number of zones (Figure 17): 322 ppm U in three samples from 11 to 12.5 m depth; 680 ppm U in four samples from 21.6 to 22.6 m; 592 ppm U (1146 ppm maximum) in six samples from 29.3 to 35.0 m; and 1824 ppm U in four samples from 38.7 to 42 m (2691 ppm maximum), but including one low value of 64 ppm.

Assessment of mean uranium grades is again difficult as uncertainty exists in estimating equilibrium levels at unsampled points. Equilibrium values in samples from 21 to 41.5 m range from 1.15 to 1.69 (Figure 17), indicating a fair attainment of equilibrium. Using these equilibrium figures, analysed uranium and calibrated gamma log values, the mean grade of uranium lies between 700 and 900 ppm over the interval from 21 to 33.5 m. Equilibrium values of 1.15 and 1.61 occur in two samples from 38 to 41 m, corresponding to a mean log value of 0.6 mR/h (0.9 mR/h maximum) (Figure 17). From these figures and the analysed uranium values, a mean grade of 2500 ppm is estimated for this 3 m length of core. The minimum assessment, assuming only perfect equilibrium (= 1.0), would be 2000 ppm U.

The uranium values are encouraging, especially as technical problems stopped the borehole some 20 m short of a presumed sub-vertical axis beneath the central part of the surface radiometric anomaly. Further mineralisation could be expected beyond the abandonment point (Figure 20).

Among the other metals (Figure 19), higher copper contents are associated generally with high uranium values, probably due to their combination in torbernite. The mean values are 220 ppm Cu (310 ppm maximum) in three samples from 11 to 12.5 m depth and 230 ppm Cu (345 ppm maximum) in five samples from 29.3 to 30.5 m. Maxima of 2000 ppm Cu occur at 34.8 to 35.4 m, and 1650 ppm Cu at 41.8 m. Mean grade is 680 ppm Cu in nine samples from 34.8 to 45.7 m depth.

Tin values reach a maximum of 435 ppm at 22.6 m depth but show little pattern. Overall mean grade in the core is 170 ppm Sn. Zinc levels are variable, but show some correlation with uranium and copper values. Five samples from 11 to 13.4 m have a mean of 410 ppm Zn (660 ppm maximum) and are associated with low amplitude uranium anomalies. A maximum of 1000 ppm Zn occurs at a depth of 34.8 m associated with a large copper value. Lead values are low. A maximum of 70 ppm Pb corresponds to the zone of uranium minerals at 42 m (Figure 19).

MINERALOGY

The main lithologies are calc-silicate rocks altered to aggregates of clay minerals and amorphous iron oxides, hard flinty quartzitic rocks and vein quartz. Brecciation is common, with deposition of chalcedonic silica and iron and manganese oxides and hydroxides.

Meta-autunite and torbernite form coatings of platy crystals on fracture surfaces, disseminated flecks within veins of chalcedony, or thin veins and stringers either traversing the rock in a sinuous network or following tension fractures in small scale folds. Autoradiography indicates some additional uranium possibly adsorbed on ferruginous material with which the uranium secondary minerals are associated. No primary uranium oxides have been found in heavy mineral separates, which consist mainly of green uranium secondary minerals, magnetite, pyrite and garnet.

Semi-quantitative X-ray fluorescence analysis of some rock samples indicates enhancements of barium (accounted for by barite), bismuth adsorbed by lithiophorite (a lithium manganese oxide/

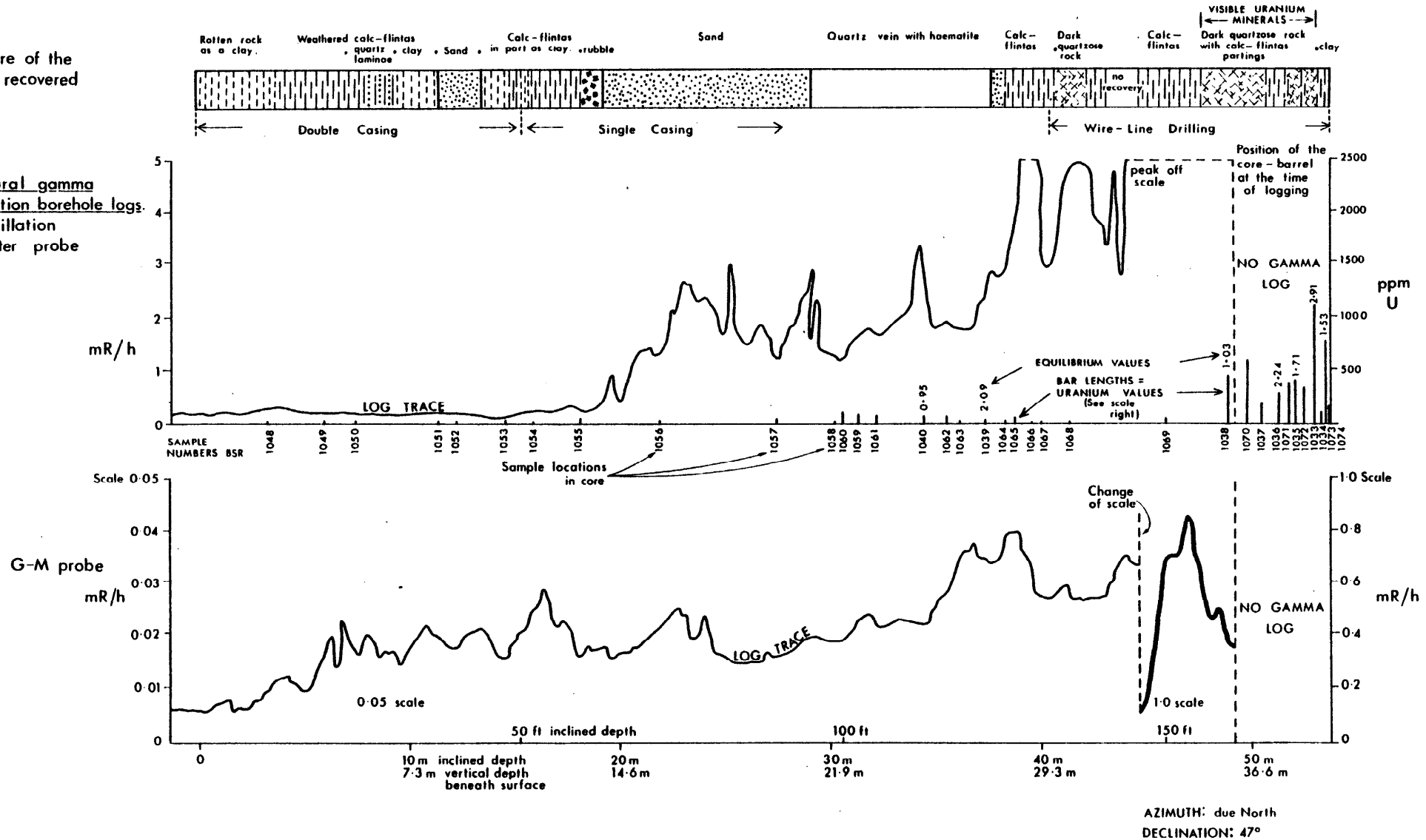

Figure 16. Radiometric logs and uranium values, Tremayne borehole No 1.

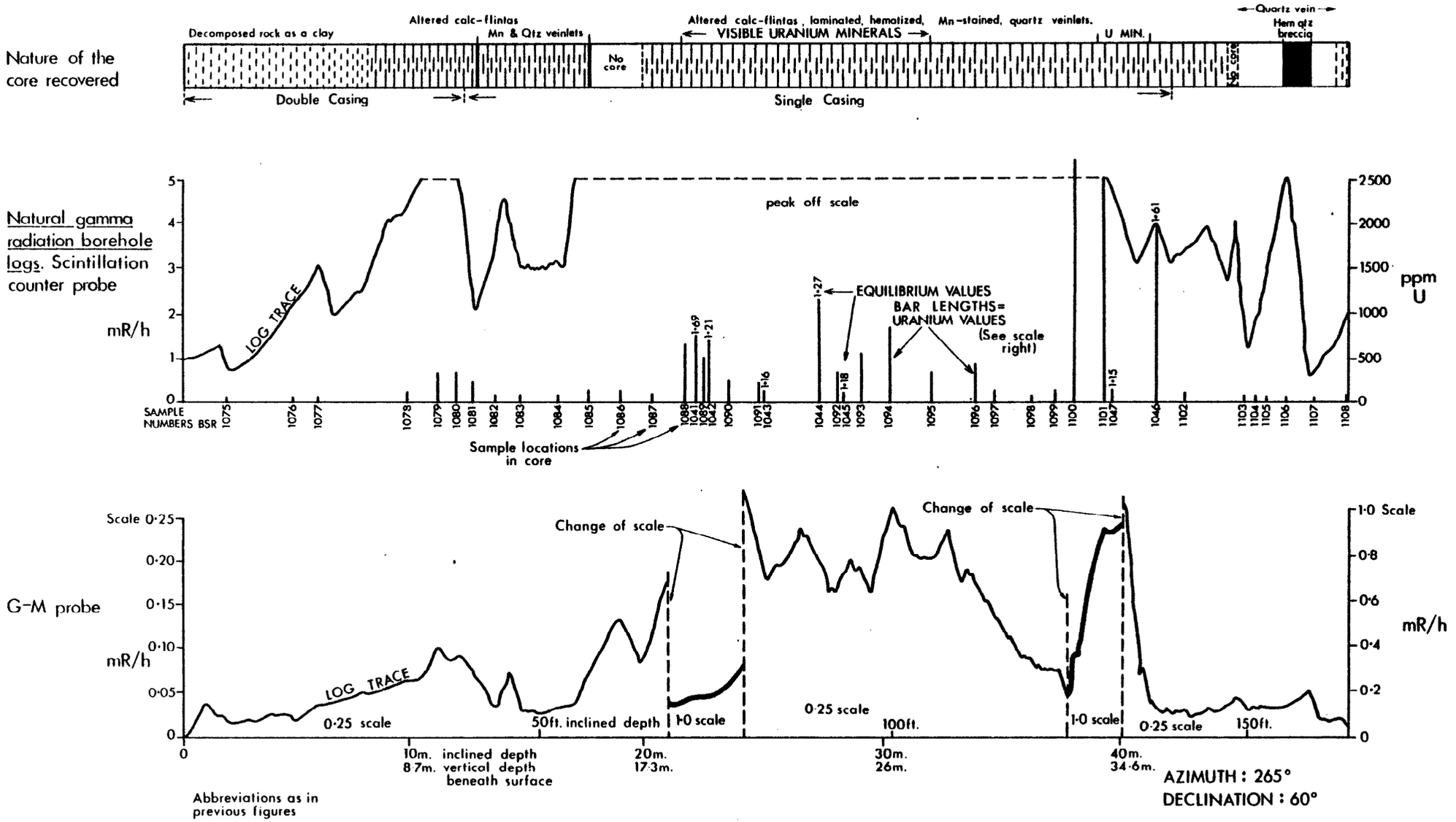

Figure 17. Radiometric logs and uranium values, Tremayne borehole No 2.

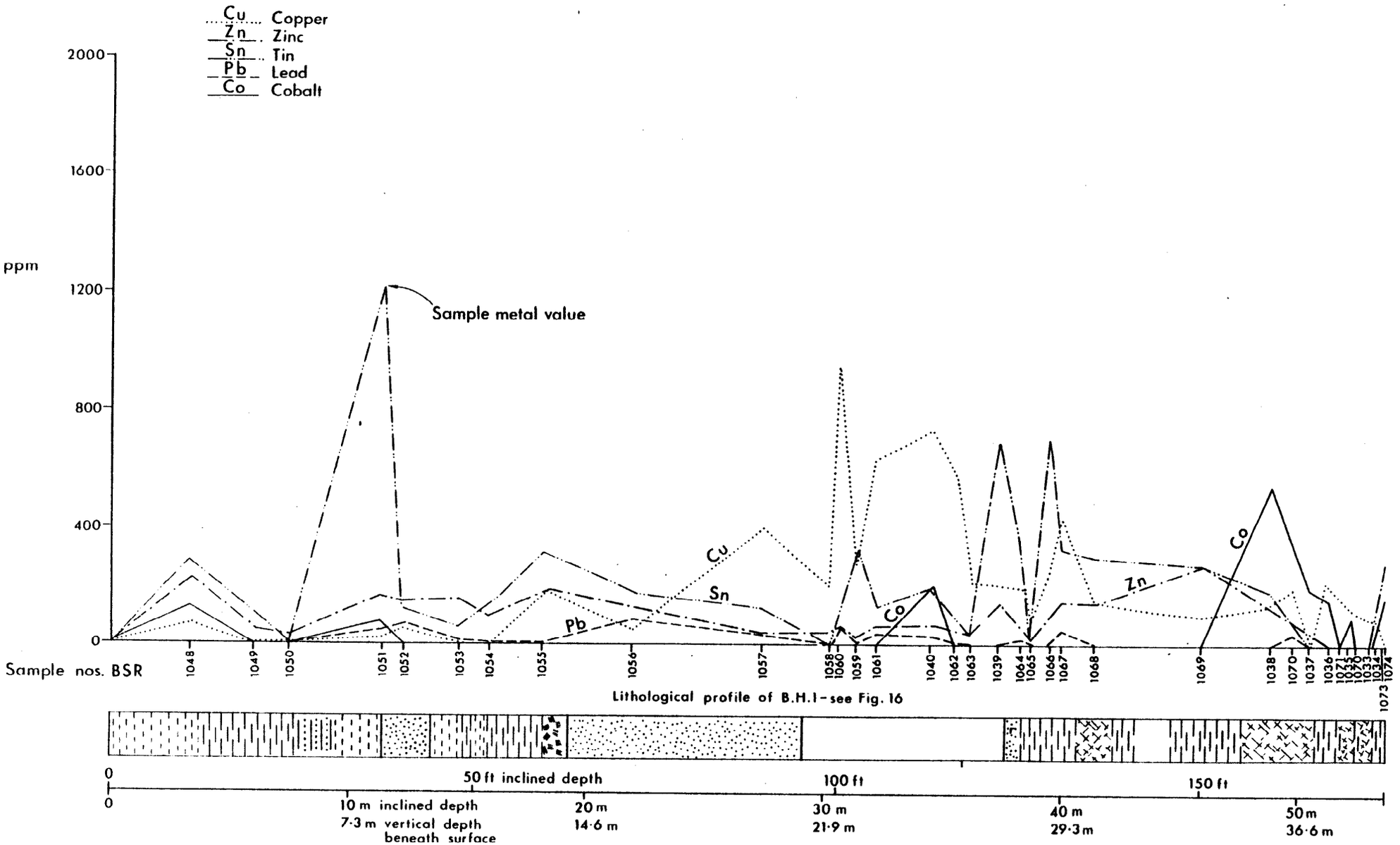

Figure 18. Metal values, Tremayne borehole no. 1

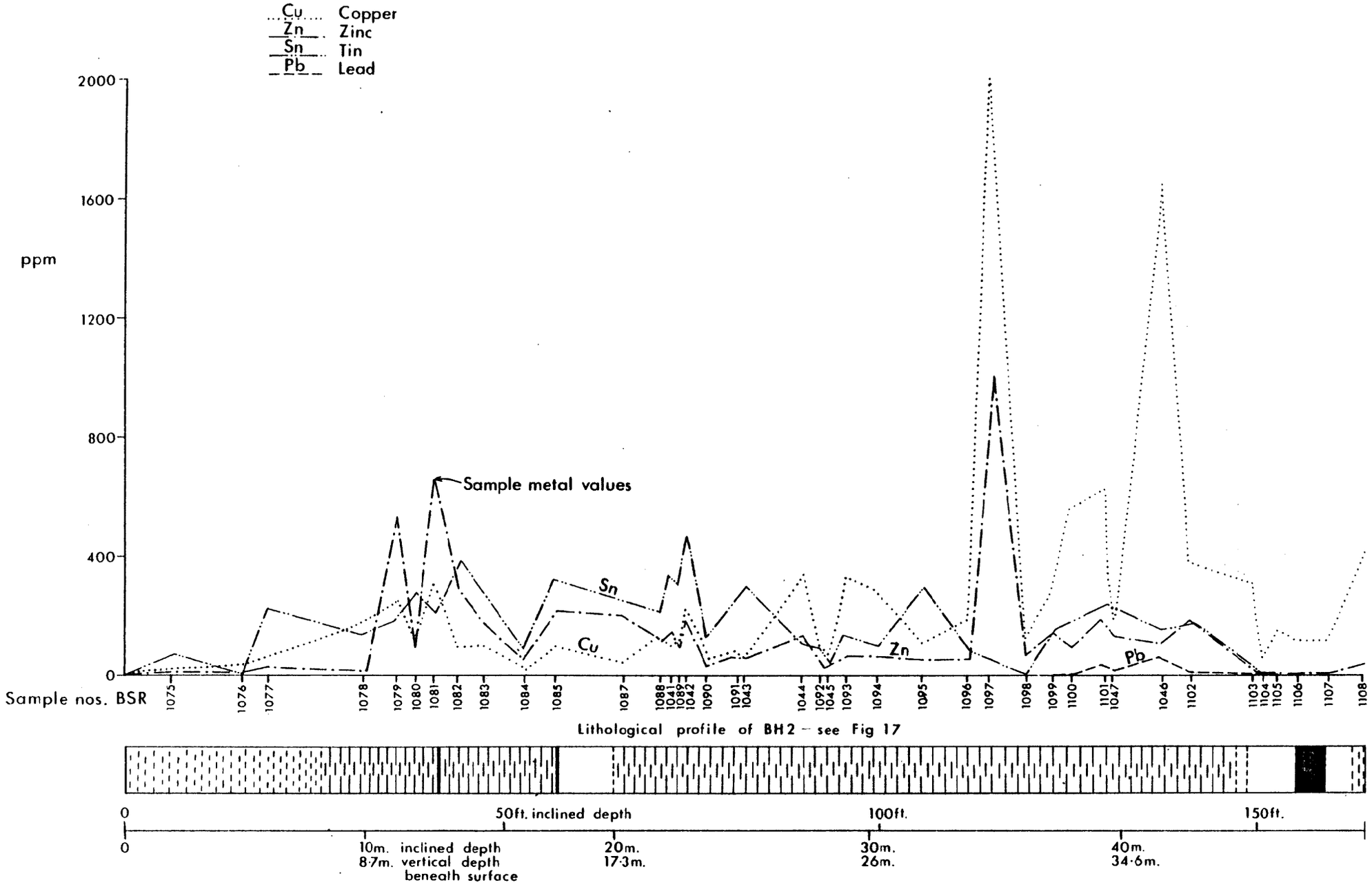

Figure 19. Metal values, Tremayne borehole no. 2

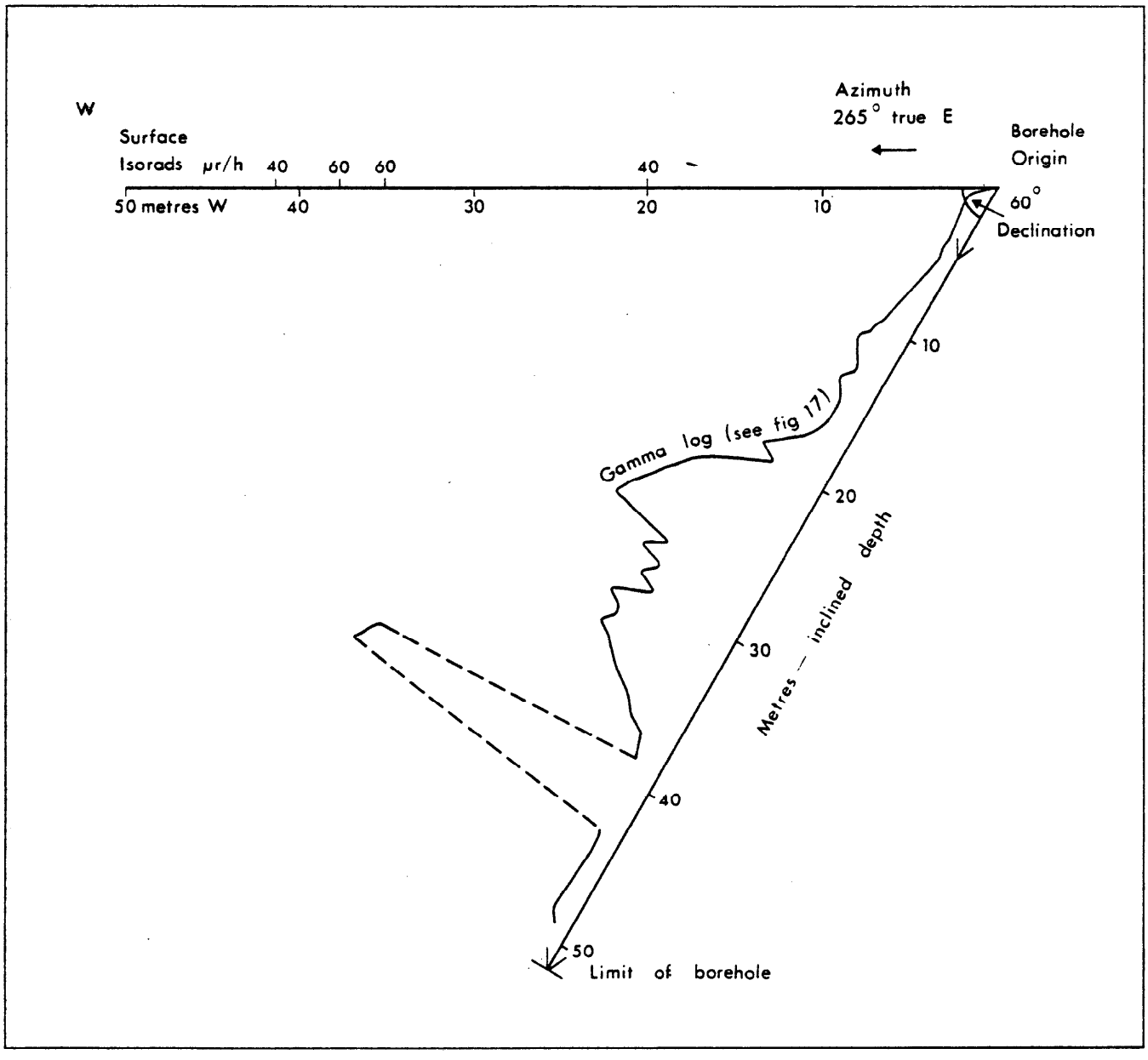

Figure 20. Diagrammatic profile and gamma log of Tremayne borehole no. 2.

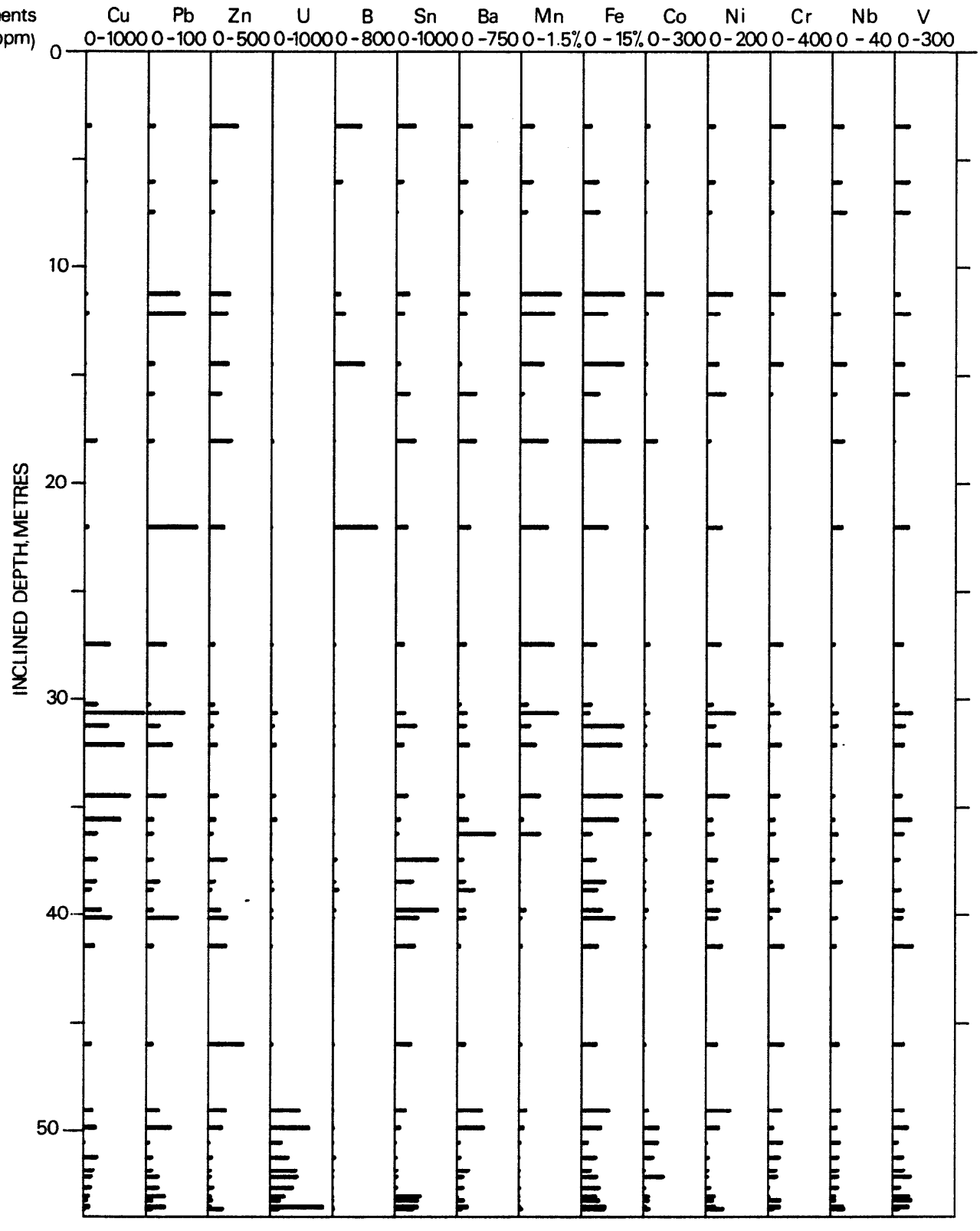

Fig. 21, Analytical Log of BH 1

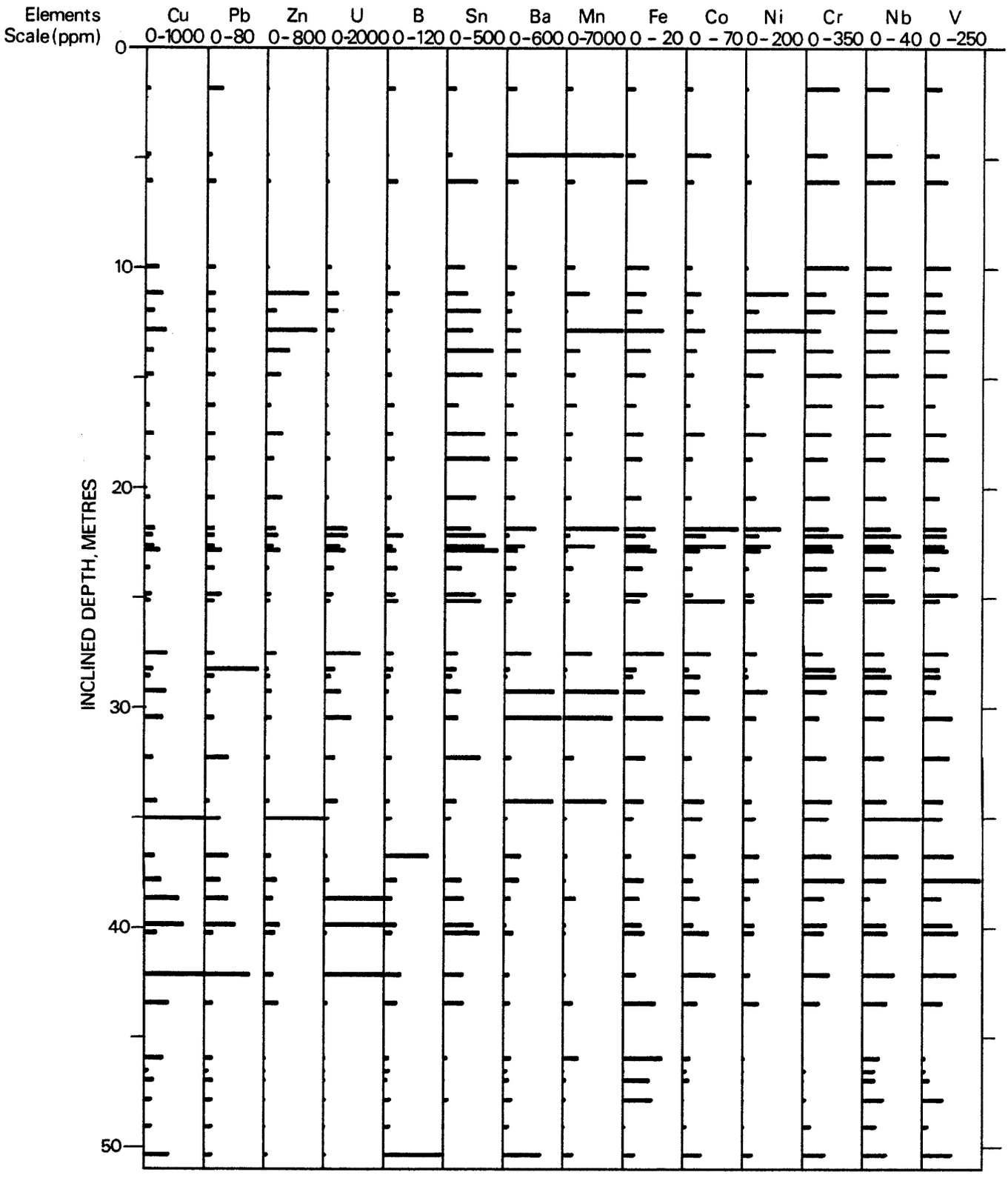

Fig. 22, Analytical Log of BH2

hydroxide), manganese in secondary minerals, and copper, adsorbed by manganese minerals or present in torbernite. No cassiterite was observed in heavy mineral separations from samples containing high tin values, and it is possible that the tin is held in grossular garnet or as malayaite, both of which are typically skarn minerals. Magnetite, pyrite and hematite are the only opaque minerals.

DISCUSSION AND CONCLUSIONS

Northerly trending faults are thought to control the uranium-copper mineralisation at Tremayne. The faulting, which post-dates the folding, has produced a belt of ground at least 200 m wide which has been brecciated, veined with quartz, hematitised and intensely decomposed. The surface radiometric anomaly coincides with this shatter belt, and primary uranium mineralisation may occur at depth within this structure. Uranium values are apparently low near the surface due to leaching and removal but may conversely be enhanced at depth due to secondary deposition.

The conservative mean grade of 0.2% U assessed in the zone towards the bottom of the second borehole, assuming that this grade alone is representative of the ground underlying the surface anomaly, may indicate the possible minimum mass of uranium ore. Between 0.3×10^6 and 0.5×10^6 tonnes of ore may exist in the volume bounded by the 40 μR/h isorad at surface, vertically down to a depth of say 60 m, which, at a grade of 0.2% U, would contain 600 to 1000 tonnes of uranium.

If the mineralised structure is sub-vertical, grades could increase considerably inwards to the centre of the anomaly, beyond the point reached by the borehole. Unless there is significant supergene enrichment, grades could also increase with depth into a primary orebody.

The intersection with low-grade uranium towards the bottom of the first borehole and the total size of the radiometric anomaly at surface may reflect the presence of a larger orebody occupying at least half the surface area bounded by the 15 μR/h isorad, of unknown depth, and with a mean grade of the order of 0.05% U. These assessments are based on the tentative interpretation of the borehole log data, and assume continuity of favourable conditions for uranium mineralisation in depth.

In Cornish uranium veins, pitchblende generally occurs with spotty sulphides, iron oxides and chalcedony or jasper, as narrow veinlets in brecciated host rock. The location of the Tremayne structures within shatter zones implies that significant mineralisation may be confined to the more competent strata such as the calc-flintas. These rocks shatter cleanly to provide an open breccia highly permeable to mineralising fluids. The deposit may, therefore, have a lithologically controlled form. An additional indication is that about 6 km to the east of Tremayne an iron lode trends N 10° W in slates and calc-flintas. In the northern part, where it cuts the calc-flintas, radioactive ferruginous fragments were located on the dumps of the Wheal James mine. Pitchblende occurs with botryoidal hematite and associated manganese oxides, chalcopyrite, marcasite and trace galena. Quartz veinlets are pseudomorphous after carbonate.

With regard to tin, in a similar but undecomposed environment in the Meadfoot Beds at Mulberry Down, 9 km east of Tremayne, cassiterite occurs as fine veinlets and disseminations within a N-S zone of boron metasomatism. This zone is close to, but not coincident with, a N-S trending hematite lode which marks a major line of movement. At Wheal Prosper, just south of Mulberry, a similar tin stockwork has been exploited but trends almost E-W. The tin mineralisation is cut by N-S quartz veins with hematite.

At Tremayne, tin values in the boreholes generally failed to fulfil the original expectations encouraged by high values in soil and trench samples. Intersections with possible tin zones at depth may not have been reached because of the abandonment of drilling before reaching target depths. Therefore, low grade economic tin mineralisation still remains a possibility and any further drilling should examine potential structures, which could be either N-S or E-W. Lack of cassiterite from cores with high tin values indicates that the metal is held in silicate phases and may have been derived from syngenetic or metasomatic enrichments.

RECOMMENDATIONS

Further drilling at the Tremayne radiometric anomaly is strongly recommended. Air-flush percussion drilling should be undertaken first, primarily to ascertain the shape, width and grades of the uranium mineralisation. Although this type of drilling can normally only be used down to the water table, its cheapness, speed and mobility make it a valuable precursor to more expensive deep core drilling. This drilling method produces rock chippings and powder for analysis and mineralogical examination and, usually, a stable hole for radiometric logging.

The technical problems of core drilling through these altered rocks are considerable. A powerful drill with large core diameter may have to be used, possibly with air-flush percussion drilling through the softer near-surface material followed by rotary, water-flush drilling for the zones beneath. This would entail recovery of only chip and dust samples in the upper part. Otherwise, inclined boreholes may need to be started outside the zones of deep surface weathering, to be determined by

geophysical and/or mechanical augering methods. As the fields are cultivated, drilling may need to be restricted to the winter period.

Further work on the other radiometric anomalies is also recommended in the light of results at Tremayne. This should comprise a pattern of air flush percussion holes and limited core drilling to obtain fresh material for examination and analysis.

The local rock units should be sampled for geochemical and mineralogical studies to identify any possible lithological control for the polymetallic mineralisation.

ACKNOWLEDGEMENTS

Thanks are due to Mr C. B. Campbell, Dr T. K. Ball, Mr K. E. Beer and Mr A. J. J. Goode, who collaborated in these investigations.

REFERENCES

Dearman, W. R. 1963. Wrench-faulting in Cornwall and South Devon. *Proc. Geol. Assoc.*, Vol. 74, pt. 3, pp. 265–287.

Dewey, H. 1925. The mineral zones of Cornwall. *Proc. Geol. Assoc.*, Vol. 74, pp. 107–135.

Dines, H. G. 1956. The metalliferous mining region of south-west England. *Mem. Geol. Surv. G.B.*, Vol. II, pp. 511–531.

El Sharkawi, M. A. H. and Dearman, W. R. 1966. Tin-bearing skarns from the north-west border of the Dartmoor Granite, Devonshire, England. *Econ. Geol.*, Vol. 61, pp. 362–369.

Freshney, E. C. 1965. Low angle faulting in the Boscastle area. *Proc. Ussher Soc.*, Vol. 1, pt. 4, pp. 175–180.

Tandy, B. C. 1974. Radiometric anomalies near St Columb Major, Cornwall. *Inst. Geol. Sci., Geochemical Division, Radioactive and Metalliferous Minerals Unit Report*, No. 322, (unpubl.).

Ussher, W. A. E., Barrow, G. and MacAlister, D. A. 1909. Geology of the country around Bodmin and St Austell. *Mem. Geol. Surv. G.B.*

APPENDIX I

BOREHOLE LOGS

Borehole 1. Azimuth 000°, Inclination -47°

This borehole was intended to identify the cause of a high soil tin anomaly (>600 ppm) but, owing to technical difficulties, the projected depth was not achieved.

Poor core recovery (approx. 30%), resulting from the highly rotten condition of the calc-silicate rocks, prevented the presentation of an accurate, detailed, lithological log. The intense decomposition encountered in this part of the outcrop was unexpected because, in contrast, the same lithology nearby has been extensively worked as a road-stone aggregate. Borehole 1 was abandoned at 53.75 m still in decomposed calc-silicate rock.

Beneath 0.91 m of brown, clayey, loamy soil and sub-soil the head deposit is represented by 2.60 m of light brown clay containing small fragments of weathered calc-silicate rocks and quartz.

Down to 28.35 m the calc-silicate bedrock is characteristically pale yellow, very soft and crumbly. More indurated sections contain intercalated fine quartz laminae, e.g. at 7.01–7.31 m and 10.82–11.43 m; elsewhere there are slaty interleaves, e.g. 17.98–19.05 m. Black manganese oxide button replacement and staining is common throughout the core, lining joints and coating cleavage surfaces. Few of the constituent calc-silicate minerals are determinable in hand specimen, though occasional yellowish green epidote-rich bands are distinguishable. Some foliation and kink-banding is also evident.

An incomplete recovery of quartz-hematite vein material begins at 28.65 m with a ferruginous sandy sludge, and from 29.87 to 37.41 m there is core of vein quartz and hematite, some of which is a bladed replacement after specularite. At 34.41 m, later quartz can be seen to re-cement joints in the quartz-hematite structure. Some of this later quartz is itself hematite-stained, subhedral and notably smoky. Crystalline quartz also lines many vughs throughout the vein.

Below 37.41 m the decomposed calc-silicate rocks are mainly hematite-stained and several joint surfaces, apparently well slickensided, are lined by green chlorite. Kink banding is clearly displayed in hematitised argillaceous calc-silicate between 38.10 and 38.63 m. Down to 47.40 m the slaty laminae are less frequently developed but quartzitic layers may be present in association with incipient silicification.

Well silicified slates occur below 47.40 m and from 51.51 to 52.58 m they become progressively more hematitised and brecciated and are re-cemented by quartz. It is within this rock that the presence of apple-green secondary uranium minerals is first noted. Meta-autunite and meta-torbernite are best developed as linings on joints and cleavages between 52.58 and 53.11 m in a zone of intensely hematitised and somewhat silicified slate.

Greenish coloured calc-silicate rocks reappear below 53.11 m and continue to the base of the hole at 53.75 m. Little meta-torbernite is seen in this section.

Borehole No. 1

Inclined depth (m)	*True depth (m)*	*Recovery*	*Lithology*
0–4.3	0–3.1	10%	Iron-stained sand, clay head.
4.3–11.4	3.1–8.3	10%	Weathered banded calc-flintas clay.
11.4–13.4	8.3–9.8	10%	Quartz, felspar and iron oxide sand.
13.4–15.9	9.8–11.6	10%	Yellow-green banded clay rubble.
15.9–19.1	11.6–14.0	10%	Fractured, iron-stained calc-flintas. Some tourmalinisation and silicification of laminae.
19.1–28.9	14.0–21.2	10%	Fine yellow-brown sand. Maroon sand in lowest 3.05 m.
28.9–37.6	21.2–27.5	50%	Quartz-tourmaline-iron oxide vein, deeply weathered and fractured. Smoky quartz.
37.6–38.6	27.5–28.2	90%	Deeply weathered and finely laminated calc-flintas.
38.6–39.4	28.2–28.8	100%	Fractured silicified calc-flintas.
39.4–40.6	28.8–29.7	40%	Deeply weathered calc-flintas.
40.6–43.1	29.7–31.5	50%	Iron and manganese oxide stained and fractured silicified rock in upper part; deeply weathered banded calc-flintas in lower part.
43.1–44.4	31.5–32.5	No recovery	
44.4–47.4	32.5–34.7	15%	Banded calc-flintas fragments.
47.4–50.5	34.7–36.9	10%	Quartzose and silicified fragments with uranium secondary minerals.
50.5–52.6	36.9–38.5	20%	As above.
52.6–53.7	38.5–39.2	95%	Dark quartzose rock in upper part, laminated clay in lower. Uranium secondary minerals.

Borehole 2. Azimth 265°, Inclination -60°

The purpose of this borehole was to intersect the N-S quartz veins identified in Trenches A and B and to investigate the near-coincident radiometric anomaly. The borehole was terminated at about half its intended length due to the technical difficulties of drilling through heavily decomposed strata cut by well-broken quartz veins. An overall core recovery of some 35% emphasises the rotten nature of the rocks encountered.

Soil and sub-soil is 0.91 m thick and consists of loam and clayey loam. This is underlain by 3.97 m of light brown clayey head which incorporates rubble of broken calc-silicate rocks and vein quartz.

The bedrock is a banded and laminated, light greenish yellow calc-silicate rock in which the joints and cleavage surfaces are commonly hematitic. Button-like black manganese oxide replacements occur widely but narrow quartz veins infilling the prominent joints are more scattered, e.g. 14.48 m. At 16.00 m finely laminated calc-silicate rocks are cut by a darkened (smoky?) quartz vein. Small flecks of meta-torbernite and meta-autunite occur on joint and cleavage surfaces between 21.49 and 31.78 m and again between 39.00 and 41.91 m.

Hematitisation increases in intensity below 36.88 m and at 45.52 m a small saccharoidal quartz vein carries red hematite and smoky quartz. Between 46.79 and 48.77 m there is brecciated vein quartz cemented by earthy red hematite. Below this breccia the quartz vein is less broken and is purer, in part chalcedonic with a few vughs lined by euhedral quartz crystals.

From 49.38 m to the bottom of the hole, at 50.44 m, the core consists of brown to yellow, altered calc-silicate rocks, partially silicified and cut by narrow (10 mm) quartz-hematite veinlets.

Borehole No. 2

Inclined depth (m)	*True depth (m)*	*Recovery*	*Lithology*
0–4.9	0–4.2	50%	Light brown clay with grit particles (altered calc-flintas). Decomposed manganese oxide rich zone at 4.7–4.9 m. Head.
4.9–7.9	4.2–6.8	40%	Light brown clay with grit particles and whitish and reddish alteration (altered calc-flintas).
7.9–11.0	6.8–9.5	30%	As above (altered calc-flintas).
11.0–12.8	9.5–11.1	66%	Decomposed calc-flintas (light green) with dark laminae and red staining. Manganese oxide lining joints at 12.5–12.8 m.
12.8–13.8	11.1–12.0	80%	As above.
13.8–15.0	12.0–13.0	40%	As above with manganese oxide and quartz veinlets along joints.
15.0–16.0	13.0–13.9	80%	As above.
16.0–17.7	13.9–15.3	40%	Hard, broken, finely laminated green calc-flintas with quartz veinlets (some dark). Some decomposed green calc-flintas. Red clay at 17.4–17.7 m.
17.7–20.0	15.3–17.3	No recovery	
20.0–21.5	17.3–18.6	25%	Hard, finely laminated calc-flintas and ?slates. Silicified.
21.5–22.4	18.6–19.4	40%	Laminated calc-flintas. Manganese oxide cement and darkened quartz in places. Some hematitisation and secondary uranium minerals in joints.
22.4–23.7	19.4–20.5	50%	Silicic laminated calc-flintas. Hematite stained. Secondary uranium minerals.
23.7–26.7	20.5–23.1	10%	Shattered. Calc-flintas laminae sub-parallel to azimuth. Green and red-stained. Some vein quartz and secondary uranium minerals.
26.7–28.4	23.1–24.6	20%	As above. Little secondary uranium.
28.4–29.3	24.6–25.3	80%	As above. Secondary uranium minerals at top.
29.3–31.8	25.3–27.5	20%	Hematitised, silicified, laminated (ruck folds) calc-flintas. Manganese oxide staining. Some secondary uranium minerals.
31.8–32.8	27.5–28.4	15%	As above, but no secondary uranium.
32.8–33.7	28.4–29.2	40%	As above.
33.7–35.0	29.2–30.3	10%	Laminated silicified calc-flintas. Manganese oxide staining.
35.0–35.4	30.3–30.7	30%	Hard silicic calc-flintas in upper part. Soft limonitic and hematitic clay in the lower part.
35.4–36.9	30.7–32.0	40%	Soft, banded calc-flintas, green to grey. Hematitic in the lower part.
36.9–39.0	32.0–33.8	60%	Friable hematitic calc-flintas. Green clay in the centre.
39.0–41.9	33.8–36.3	10%	Hard banded calc-flintas rubble. Hematitic and limonitic. Secondary uranium minerals towards the bottom.

Inclined depth (m)	*True depth (m)*	*Recovery*	*Lithology*
41.9–45.1	36.3–39.1	10%	Hard hematitised banded calc-flintas. Manganese oxide-stained.
45.1–45.5	39.1–39.4	No recovery	
45.5–45.8	39.4–39.7	90%	Quartz vein with clear, milky and smoky quartz in a number of generations. Iron and manganese oxide-stained.
45.8–46.8	39.7–40.5	50%	As above.
46.8–47.7	40.5–41.3	90%	As above, hematitised quartz breccia towards the bottom.
47.7–48.8	41.3–42.3	40%	Hematitised quartz breccia.
48.8–48.9	42.3–42.4	100%	Quartz vein.
48.9–49.0	42.4–42.5	100%	As above.
49.0–49.4	42.5–42.8	100%	As above.
49.4–50.5	42.8–43.7	70%	Quartz vein at the top with yellow-brown altered calc-flintas, with small quartz/hematite veinlets. Manganese oxide on joints.

APPENDIX II

ANALYTICAL AND STATISTICAL DATA

Samples were analysed for uranium by the delayed neutron method at the Atomic Weapons Research Establishment, Aldermaston; for copper, lead, zinc and silver by atomic absorption spectrophotometry and for other elements (listed in Table 2) by optical omission spectroscopy, at the Analytical Chemistry Unit (ACU) of the Institute of Geological Sciences.

Total analytical results are not reproduced here. Salient element contents are recorded in the text and illustrations. The full results are held within the IGS computer data base and are available on request.

Some standard statistical extracts from log-treated histograms, cumulative frequency curves and correlation matrices are presented below.

Soil samples

Samples were collected on a grid pattern, the origin of which is shown in Figure 4. Sample positions are recorded in computer-merged data in metres east and north of the origin by positive figures, and metres west and south by negative values, along lines perpendicular to and parallel to the base line.

Figures 8 and 9 illustrate analytical values for uranium, tin, copper, lead and zinc. Table 1 sets out data too congested to show along the line of the Water Board trench in Figure 8, and Tables 2 and 3 present statistical summaries of the data from all the soil samples.

Table 1 Analytical results from soil samples from Water Board trench

	Depth	*Metres east* (grid origin shown fig. 4)	*Metres north*	*Copper ppm*	*Lead ppm*	*Zinc ppm*	*Uranium ppm*	*Tin ppm*
AZ8217	All at	35	-185	20	30	70	2.9	42
8218	1.5 m unless	40	-185	15	30	50	2.9	32
8219	otherwise	45	-185	15	20	80	3.4	18
8220	stated	50	-185	25	20	80	2.6	32
8221		55	-185	10	20	80	2.3	3
8222		60	-185	15	30	140	2.4	4
8223		65	-185	5	20	100	3.4	3
8224		70	-185	15	30	120	3.8	56
8246		26	-185	35	20	90	11.1	42
8247		25	-185	45	20	80	10.5	42
8248		24	-185	90	20	30	11.1	42
8249		23	-185	165	30	20	19.0	180
8250		22	-185	460	160	70	22.9	56
8251		21	-185	990	240	110	3.6	100
8252		20	-185	240	70	40	7.9	100
8253		19	-185	120	20	30	7.5	10
8254		18	-185	45	10	20	7.7	32
8255		17	-185	70	20	20	10.4	42
8256		16	-185	110	20	20	8.3	130
8257		15	-185	75	10	20	7.5	180
8258		14	-185	130	20	40	5.9	56
8259		13	-185	45	10	10	5.2	10
8260		12	-185	170	20	30	7.5	75
8261		11	-185	200	10	50	8.7	18
8262		10	-185	160	20	54	16.7	56
8263		9	-185	245	10	50	9.0	8
8264		8	-185	135	10	60	12.6	8
8265		7	-185	125	10	40	19.1	24
8266		6	-185	105	10	40	11.3	24
8267		5	-185	170	10	90	13.1	18
8268		4	-185	110	10	150	14.5	24
8269		3	-185	170	20	50	29.5	75
8270		2	-185	225	20	50	79.5	13
8271	(0.7 m)	2	-185	130	20	50	11.7	13
8272		1	-185	150	20	40	27.2	42
8273	(0.7 m)	1	-185	200	20	40	22.1	18
8274		0	-185	170	30	50	22.2	6
8275	(0.7 m)	0	-185	125	20	30	31.2	42
8276		-1	-185	200	20	40	28.5	3
8277	(0.7 m)	-1	-185	140	30	30	76.2	56
8278		-2	-185	170	20	30	45.7	6
8279	(0.7 m)	-2	-185	220	40	40	154.0	42
8280		-3	-185	190	20	30	53.2	8
8281	(0.7 m)	-3	-185	380	40	70	155.0	56
8282		-4	-185	370	50	50	277.0	18
8283	(0.7 m)	-4	-185	120	20	60	24.3	10
8284		-5	-185	200	40	60	41.5	2
8285	(0.7 m)	-5	-185	240	30	70	33.8	1
8286		-6	-185	205	40	40	204.0	24
8287	(0.7 m)	-6	-185	100	20	50	60.0	2
8288		-7	-185	175	10	50	252.0	56
8289	(0.7 m)	-7	-185	110	20	50	140.0	32
8290		-8	-185	70	10	50	146.0	18
8291	(0.7 m)	-8	-185	70	20	50	134.0	42
8292		-9	-185	75	20	100	62.7	3
8293	(0.7 m)	-9	-185	90	10	60	133.0	100
8294		-10	-184	55	20	60	42.1	3
8295		-11	-184	20	10	50	48.3	10
8296		-12	-184	15	10	60	35.0	18
8297		-13	-184	30	20	70	46.6	18
8298		-14	-184	55	20	70	35.6	10
8299		-15	-184	35	20	60	41.5	18
8500		-16	-183	30	20	80	39.3	42
8501		-17	-183	50	20	80	25.9	18
8502		-18	-183	35	20	60	15.1	18
8503		-19	-183	40	10	70	27.6	32
8504		-20	-183	45	30	80	27.9	32
8505		-21	-182	45	30	70	15.6	32
8506		-22	-182	80	20	70	17.1	32
8507		-23	-182	55	40	70	14.8	18
8508		-24	-182	40	20	70	12.7	24
8509		-25	-182	35	10	80	11.2	24
8510		-26	-182	40	30	70	12.0	13
8511		-32	-180	25	10	70	7.3	8
8512		-37	-179	10	20	70	3.6	13
8513		-42	-178	35	20	70	3.4	42
8514		-46	-176	20	20	80	3.7	13
8515		-51	-175	25	20	80	3.7	10
8516		-56	-174	25	30	100	3.1	18
8517		-61	-173	20	10	80	3.7	8
8518		-65	-171	20	10	60	3.7	6
8519		-70	-170	35	20	80	3.1	18
8520		-75	-168	75	30	90	2.0	10
8521		-80	-167	15	10	70	3.4	18
8522		-85	-166	20	20	70	3.3	13
8523		-89	-164	25	20	60	3.1	18
8524		-94	-163	20	10	80	3.0	6
8525		-98	-161	35	20	80	3.5	56
8526		-103	-160	10	10	70	3.2	32
8527		-108	-158	30	10	100	2.9	24
8528		-113	-157	20	30	90	2.9	32
8529		-118	-156	15	10	90	2.9	32
8530		-123	-155	15	10	120	3.3	18
8531		-128	-153	60	10	90	2.1	100
8532		-133	-152	10	0	70	1.3	180
8533		-138	-151	10	10	70	3.5	6
8534		143	-150	20	10	100	2.8	10

Table 2 Statistical summary of soil sample analyses (n = 121)

Element	*Limits*		*Mean*	*Mode*	*Median*	*Class break*
	Lower	*Upper*	*(geometric)*			*and percentile*
Copper	0.0	990	30	20	25	Log-normal
Lead	0.0	240	19	20	20	Log-normal
Zinc	10.0	400	72	90	70	Log-normal
Uranium	1.0	277	6.2	4.0	3.7	3.86 (60%)
Boron	0.0	10 000	18	158	56	–
Tin	0.0	560	15	23	18	Log-normal
Manganese	0.0	3.2	0.135	0.084	0.13	Log-normal
Iron	0.0	42.0	9.12	6.03	10.0	–
Cobalt	0.0	180	21	29	24	–
Nickel	0.0	320	63	42	56	–
Molybdenum	0.0	10	1.1	–	–	–
Barium	0.0	1800	78	190	180	–
Vanadium	0.0	420	132	170	130	–
Chromium	0.0	420	141	170	180	–
Yttrium	0.0	750	12	28		12 (50%)
Niobium	0.0	75	2.2	60	–	–

Figures in ppm except manganese and iron (per cent). Figures to nearest significant number from log-transformed data.
– indicates insufficient or inprecise data.

Table 3 Correlation strength matrix for soil sample values (n = 121)

Element		*Cu*	*Pb*	*Zn*	*U*	*B*	*Sn*	*Mn*	*Fe*	*Co*	*Ni*	*Mo*	*Ba*	*V*	*Cr*	*Y*	*Nb*
Copper	Cu	9	3	0	5	1	2	0	1	0	-1	1	-2	0	0	1	0
Lead	Pb	3	9	3	0	-1	1	0	0	1	0	1	0	0	-1	-3	0
Zinc	Zn	0	3	9	-2	-2	0	2	1	0	2	2	0	0	-1	-3	0
Uranium	U	5	0	-2	9	0	0	0	0	1	-1	0	-1	0	1	1	0
Boron	B	1	-1	-2	0	9	0	1	0	2	0	-1	2	0	1	4	0
Tin	Sn	2	-1	0	0	0	9	5	3	0	-1	2	-4	-1	0	0	0
Manganese	Mn	0	0	2	0	1	5	9	2	4	4	2	-1	2	3	0	0
Iron	Fe	1	0	1	0	0	3	2	9	2	2	1	0	2	2	0	0
Cobalt	Co	0	1	0	1	2	0	4	2	9	5	0	1	5	5	1	0
Nickel	Ni	-1	0	2	-1	0	-1	4	2	5	9	0	3	6	6	1	0
Molydenum	Mo	1	1	2	0	-1	2	2	1	0	0	9	-2	-1	0	-1	0
Barium	Ba	-2	0	0	-1	2	-4	-1	0	1	3	-2	9	3	1	0	0
Vanadium	V	0	0	0	0	0	-1	2	2	5	6	-1	3	9	7	1	0
Chromium	Cr	0	-1	-1	1	1	0	3	2	5	6	0	1	7	9	2	1
Yttrium	Y	1	-3	-3	1	4	0	0	0	1	1	-1	0	1	2	9	1
Niobium	Nb	0	0	0	0	0	0	0	0	0	0	0	0	0	1	1	9

Trench samples

Samples were collected on the grid pattern used for the soil samples. Salient element values are shown in the text and in Figures 12, 13 and 14. Statistical summaries are in Tables 4 and 5 below.

Table 4 Statistical summary of trench sample analyses (n = 79)

Element	*Limits*		*Mean*	*Mode(s)*	*Median*	*Class break*
	Lower	*Upper*	*(geometric)*			*and percentile*
Copper	5.0	580	85	120	90	Log-normal
Lead	0.0	50	4.3	10	10	–
Zinc	10.0	640	47	35	40	Log-normal
Uranium	1.7	408	42	50, 166	50	41 (34%)
Boron	1.0	2966	48	36	44	55 (66%)
Tin	0.0	943	65	170	112	182 (75%)
Manganese	0.0124	1.4497	0.126	0.214	0.144	Log-normal
Iron	1.2425	18.197	4.898	5.5	5.36	Log-normal
Cobalt	4.0	68	11	10	11	19.4 (91%)
Nickel	2.0	154	32	44	35	61 (76%)
Molybdenum	0.0	3	1.1	1, 2	–	–
Barium	0.0	808	76	110	92	Log-normal
Vanadium	14.0	146	69	90	77	69 (50%)
Chromium	18.0	313	145	178	156	115 (20%)
Yttrium	42.0	582	120	162	106	–
Niobium	0.0	22	15	13.8	16	–

Figures in ppm except manganese and iron (per cent). Figures to nearest significant number from log-transformed data.
– indicates insufficient or inprecise data.

Table 5 Correlation strength matrix for trench samples values (n = 79)

Element		*Cu*	*Pb*	*Zn*	*U*	*B*	*Sn*	*Mn*	*Fe*	*Co*	*Ni*	*Mo*	*Ba*	*V*	*Cr*	*Y*	*Nb*
Copper	Cu	9	2	3	5	-4	2	4	3	3	2	2	1	0	-4	3	-3
Lead	Pb	2	9	1	1	-1	2	1	2	1	2	2	0	0	-3	0	-2
Zinc	Zn	3	1	9	0	1	3	6	5	2	7	1	1	1	-2	1	0
Uranium	U	5	1	0	9	-6	1	0	2	0	0	3	0	0	-1	3	0
Boron	B	-4	-1	1	-6	9	0	2	0	0	1	-2	0	1	2	-1	1
Tin	Sn	2	2	3	1	0	9	3	5	0	1	1	0	3	0	1	2
Manganese	Mn	4	1	6	0	2	3	9	5	5	4	0	2	0	-2	0	0
Iron	Fe	3	2	5	2	0	5	5	9	1	3	3	1	3	-2	1	2
Cobalt	Co	3	1	2	0	0	0	5	1	9	5	0	1	0	-1	1	-1
Nickel	Ni	2	2	7	0	1	1	4	3	5	9	1	1	2	-1	1	2
Molydenum	Mo	2	2	1	3	-2	1	0	3	0	1	9	0	0	-2	1	1
Barium	Ba	1	0	1	0	0	0	2	1	1	1	0	9	1	0	1	0
Vanadium	V	0	0	1	0	1	3	0	3	0	2	0	1	9	3	4	6
Chromium	Cr	-4	-3	-2	-1	2	0	-2	-2	-1	-1	-2	0	3	9	1	5
Yttrium	Y	3	0	1	3	-1	1	0	1	1	1	1	1	4	1	9	2
Niobium	Nb	-3	-2	0	0	1	2	0	2	-1	2	1	0	6	5	2	9

Borehole samples

Important element values are indicated in the text and in Figures 16, 17, 18 and 19 and analytical logs in Figures 21 and 22. Statistical summaries are in Tables 6 and 7 below.

Table 6 Statistical summary of borehole sample analyses (n = 77)

Element	*Limits*		*Mean*	*Mode(s)*	*Median*	*Class break and percentile*
	Lower	*Upper*	*(geometric)*			
Copper	5.0	2000	129	140	130	Log-normal
Lead	5.0	80	14	10	10	Log-normal
Zinc	10.0	1000	66	–	70	110 (60%), 185 (92%)
Uranium	2.20	2691	89	77, 372	89	Log-normal
Boron	1.0	1383	16	13	14	26 (84%)
Tin	2.0	1203	117	204	158	240 (66%)
Manganese	0.007	1.3	0.085	–	0.075	0.51 (84%)
Iron	0.27	12.9	5.13	7.16	5.66	Log-normal
Cobalt	1.0	521	16	9	13	51 (90%)
Nickel	1.0	211	27	32	34	17 (25%)
Molybdenum	0.0	6	1.3	–	–	–
Barium	9.0	1298	91	106	91	76 (39%), 114 (83%)
Vanadium	9.0	332	79	78	86	46 (12%)
Chromium	0.0	247	102	107	124	66 (12%)
Niobium	2.0	39	15	15	15	13 (16%)

Figures in ppm except manganese, iron (per cent). Figures to nearest significant number from log-transformed data.
– indicates insufficient or inprecise data.

Table 7 Correlation strength matrix for borehole sample values (n = 77)

Element		*Cu*	*Pb*	*Zn*	*U*	*B*	*Sn*	*Mn*	*Fe*	*Co*	*Ni*	*Mo*	*Ba*	*V*	*Cr*	*Nb*
Copper	Cu	9	2	2	4	-2	0	0	2	0	1	2	0	1	-1	1
Lead	Pb	2	9	1	0	3	2	0	1	1	2	2	-1	3	1	0
Zinc	Zn	2	1	9	0	2	5	2	4	2	8	-1	0	4	3	3
Uranium	U	4	0	0	9	-2	1	-2	1	2	0	0	0	1	-1	0
Boron	B	-2	3	2	-2	9	1	1	1	1	2	-1	0	2	1	2
Tin	Sn	0	2	5	1	1	9	2	5	2	6	0	1	6	4	2
Manganese	Mn	0	0	2	-2	1	2	9	4	2	4	1	4	0	0	0
Iron	Fe	2	1	4	1	1	5	4	9	1	4	1	2	4	0	0
Cobalt	Co	0	1	2	2	1	2	2	1	9	3	2	2	1	1	4
Nickel	Ni	1	2	8	0	2	6	4	4	3	9	0	2	5	3	3
Molydenum	Mo	2	2	-1	0	-1	0	1	1	2	0	9	0	0	-2	1
Barium	Ba	0	-1	0	0	0	1	4	2	2	2	0	9	0	0	0
Vanadium	V	1	3	4	1	2	6	0	4	1	5	0	0	9	5	2
Chromium	Cr	-1	1	3	1	1	4	0	0	1	3	-2	0	5	9	2
Niobium	Nb	-1	0	3	0	2	2	0	0	4	3	1	0	2	2	9